

# Phase transitions in the early and the present Universe: from the big bang to heavy ion collisions\*

D. Boyanovsky

Department of Physics and Astronomy, University of Pittsburgh,  
Pittsburgh PA. 15260, U.S.A

October 31, 2018

## Abstract

In these lectures I discuss cosmological phase transitions with the goal of establishing the possibility of observational consequences. I argue that the *only* phase transition amenable of experimental study within the foreseeable future is that predicted by QCD and discuss some of the potential observational cosmological consequences associated with this phase transition(s). I describe the experimental effort to study the QCD phase transition(s) at RHIC and SPS and summarize some of the recent experimental results. The possibility of novel phases of QCD in the core of pulsars is discussed along with the suggested observational consequences. A brief review of standard big bang cosmology as well as the astrophysics of compact stars sets the stage for understanding the observational cosmological and astrophysical consequences of phase transitions in the standard model.

## Contents

<b>1</b>	<b>Prologue: Cosmological Phase Transitions, Theory vs. Observations</b>	<b>2</b>
<b>2</b>	<b>The Standard Hot Big Bang</b>	<b>2</b>
2.1	Ingredients . . . . .	2
2.2	The building blocks: . . . . .	3
2.3	Energy scales: . . . . .	5
<b>3</b>	<b>Phase Transitions and their aftermath</b>	<b>6</b>
3.1	GUT's and inflation . . . . .	6
3.1.1	Density perturbations and the signature of a phase transition . . . . .	8
3.2	The Electroweak Phase Transition: Baryogenesis? . . . . .	11
3.3	The QCD phase transition(s) . . . . .	12
3.4	Nucleosynthesis . . . . .	15
3.5	Recombination, LSS and CMB . . . . .	17
3.6	Galaxy formation and on to Stars... . . . .	18
3.7	Stellar Evolution 101: QGP at the core of Pulsars? . . . . .	19
3.8	Executive Summary: observational consequences of cosmological phase transitions? . . . . .	22

---

\*Lectures delivered at the Nato Advanced Study Institute: Phase Transitions in the Early Universe: Theory and Observations. Erice, 6th-17th December 2000. Eds, H. J. de Vega, I. Khalatnikov, N. Sanches.

<b>4</b>	<b>Relativistic heavy ion collisions and pulsars open a window to the early Universe:</b>	<b>22</b>
4.1	RHIC and LHC seek the QGP: the big picture . . . . .	23
4.1.1	Hydro, LGT and the EoS: . . . . .	23
4.2	Thermalization, quasiparticles and the EoS: . . . . .	26
4.3	Predictions and observations: . . . . .	27
4.3.1	$J/\Psi$ suppression: . . . . .	27
4.3.2	Electromagnetic probes: dileptons and direct photons . . . . .	28
4.3.3	Strangeness enhancement . . . . .	30
4.3.4	Collective flow and the EoS: . . . . .	31
4.3.5	Other predictions... . . . .	32
4.4	Little bang vs. Big Bang: . . . . .	33
4.5	QGP in the core of pulsars: . . . . .	34
<b>5</b>	<b>Back to the early Universe: summary</b>	<b>36</b>

# 1 Prologue: Cosmological Phase Transitions, Theory vs. Observations

The theme of this School is Cosmological Phase Transitions, Theory and Observation.

A wealth of cosmological data is providing confirmation of sound theoretical ideas in early Universe cosmology. Measurements of temperature anisotropy in the CMB by satellite, balloon borne and earth based observations as well as measurements of the acceleration of the expansion with supernovae Type Ia searches and precision measurements of light element abundances (for recent reviews see [1]) provide an impressive body of complementary high quality data.

While the unprecedented quantity and quality of cosmological data seems to validate the main ideas of early Universe cosmology, the observational consequences of cosmological *phase transitions* are still rather indirect. Although there is more theory than *direct* observation of aspects of cosmological phase transitions, I will argue in these lectures that current and future accelerator experiments along with observations of the properties of pulsars will be opening a window to the early Universe at a time scale of about  $10^{-6}$  seconds after the Big Bang.

To set the stage for the description of the experimental effort to probe the *last* phase transition predicted by the standard model of particle physics, and to understand its potential cosmological impact, I review the standard hot big bang model and the astrophysics of compact stars, emphasizing the different scales and the observations associated with relevant phenomena.

## 2 The Standard Hot Big Bang

### 2.1 Ingredients

The standard “Hot Big Bang” theory of Early Universe cosmology is based on a wealth of observations and rests upon the following pillars:

- Homogeneity and isotropy: on large scales  $\geq 100\text{Mpc}$  the Universe looks homogeneous and isotropic. This is confirmed by galactic surveys of large scale structure and by the homogeneity and isotropy of the Cosmic Microwave Background (CMB).
- The Hubble expansion: objects that are separated by a (comoving) distance  $d$  recede from each other with a velocity  $v = H d$  with  $H$  the Hubble parameter (or Hubble constant) whose value today is

$H_0 \sim 65\text{Km/s/Mpc}$ . The Hubble law of expansion determines the size of the *causal horizon*, objects separated by a comoving distance

$$d_H = 3000h^{-1}\text{Mpc} \quad (2.1)$$

$$h = \frac{H}{100\text{Km/s/Mpc}} \quad (2.2)$$

recede from each other at the speed of light and are therefore causally disconnected. In particular the size of the visible (causal) horizon today is  $\sim 3000$  Mpc.

- The fossil Cosmic Microwave Background (CMB) radiation: The Universe is immersed in a bath of thermal photons at a temperature  $T_0 = 2.73\text{K}$  with an almost perfect blackbody distribution. This distribution and small anisotropies of order  $\Delta T/T_0 \sim 10^{-5}$  were measured in 1992 by the COBE satellite and their detection represents a triumph for the standard hot big bang model [2]. The small temperature anisotropies, predicted by cosmological models, provide the clue to the origin of galaxy formation and large scale structure and is an important confirmation of theories of early Universe cosmology.
- The abundance of light elements: Observations of the abundance of elements in low metallicity regions reveals that about 76% of matter is in the form of Hydrogen, about 24% (by mass) in  ${}^4\text{He}$  and very small abundances of  ${}^3\text{He}$  ( $\sim 10^{-5}$ ), deuterium (D) ( $\sim 10^{-5}$ ) and  ${}^7\text{Li}$  ( $\sim 10^{-10}$ ) all relative to Hydrogen. These elements were formed during the first three minutes after the Big Bang, while heavier elements are produced in the interior of stars and astrophysical processes such as supernovae explosions.

## 2.2 The building blocks:

The main building blocks for a theory of the standard Hot Big Bang are:

- **Gravity:** *Classical* general relativity provides a good description of the geometry of space time for distances  $l \geq l_{Pl} \sim 10^{-33}\text{cm}$  or time scales  $t \geq t_{Pl} \sim 10^{-43}\text{s}$ , or equivalently energy scales smaller than the Planck scale  $M_{Pl} \sim 10^{19}\text{Gev}$ . We have to wait for a consistent quantum theory of gravity unified with matter to explain phenomena on shorter space-time scales or larger energy scales.

Homogeneity and isotropy lead to the Robertson-Walker metric

$$ds^2 = dt^2 - a^2(t) \left[ \frac{dr^2}{1 - kr^2} + r^2 (d\theta^2 + \sin^2(\theta) d\phi^2) \right] \quad (2.3)$$

where  $t$  is the comoving time. The constant  $k$  determines the spatial curvature and can be set to be either  $\pm 1$  or  $0$  by redefining the scale of coordinates. For  $k = 1, 0, -1$  the Universe is closed, flat or open respectively. The scale factor  $a(t)$  relates physical and comoving scales

$$l_{phys}(t) = a(t)l_{com} \quad (2.4)$$

The Friedmann equation determines the evolution of the scale factor from the energy density

$$\left( \frac{\dot{a}(t)}{a(t)} \right)^2 \equiv H^2(t) = \frac{8\pi\rho}{3M_{Pl}^2} - \frac{k}{a^2(t)} \quad (2.5)$$

A spatially flat Universe has the critical density

$$\rho_c = \frac{3}{8\pi} M_{Pl}^2 H^2 \quad (2.6)$$

and it is customary to introduce the ratio of the density of any component (radiation, matter etc) to the critical density as

$$\Omega = \frac{\rho}{\rho_c} \quad (2.7)$$

The energy momentum tensor is assumed to have the fluid form leading to the (fluid) conservation of energy equation

$$\dot{\rho} + 3(\rho + p) \frac{\dot{a}}{a} = 0 \quad (2.8)$$

where  $\rho, p$  are the energy density and pressure respectively. The two equations (2.5,2.8) can be combined to yield the acceleration of the scale factor,

$$\frac{\ddot{a}}{a} = -\frac{4\pi}{3M_{Pl}^2}(\rho + 3p) \quad (2.9)$$

which will prove useful later. In order to provide a close set of equations we must append an “equation of state”  $p = p(\rho)$  which is typically written in the form

$$p = w(\rho)\rho \quad (2.10)$$

Current observations [1] favor a spatially flat Universe  $k \equiv 0$  which is consistent with predictions from inflationary scenarios. For a spatially flat Universe  $k = 0$  and for  $w = \text{constant}$  we obtain the following important cases:

$$w = 0 : \text{Matter domination} \Rightarrow \rho \propto a^{-3} ; a(t) \propto t^{\frac{2}{3}} \quad (2.11)$$

$$w = \frac{1}{3} : \text{Radiation domination} \Rightarrow \rho \propto a^{-4} ; a(t) \propto t^{\frac{1}{2}} \quad (2.12)$$

$$w = -1 : \text{De Sitter expansion} \Rightarrow \rho = \text{constant} ; a(t) \propto e^{Ht} ; H = \sqrt{\frac{8\pi\rho}{3M_{Pl}^2}} \quad (2.13)$$

Furthermore we see that for accelerated expansion it must be the case that  $w < -1/3$ .

- **The Standard Model of Particle Physics:** the current standard model of particle physics, experimentally tested with remarkable precision describes the theory of strong (QCD), weak and electromagnetic interactions (EW) as a gauge theory based on the group  $SU(3)_c \otimes SU(2) \otimes U(1)$ . The particle content is: 3 generations of quarks and leptons:

$$\begin{pmatrix} u \\ d \end{pmatrix} \begin{pmatrix} c \\ s \end{pmatrix} \begin{pmatrix} t \\ b \end{pmatrix} ; \begin{pmatrix} \nu_e \\ e \end{pmatrix} \begin{pmatrix} \nu_\mu \\ \mu \end{pmatrix} \begin{pmatrix} \nu_\tau \\ \tau \end{pmatrix}$$

vector Bosons: 8 gluons (massless) ,  $Z_0$  (mediate neutral currents),  $W^\pm$  (mediate charge currents) with masses of order 80, 90 Gev respectively and the photon (massless) and scalar Higgs bosons, although the experimental evidence for the Higgs boson is still inconclusive.

Current theoretical ideas propose that the strong, weak and electromagnetic interactions are unified in a grand unified quantum field theory (GUT), perhaps with supersymmetry as the underlying fundamental symmetry and a unification scale  $M_{GUT} \sim 10^{15}\text{Gev}$ . Furthermore the ultimate scale at which Gravity is eventually unified with the rest of particle physics is the Planck scale  $M_{Pl} \sim 10^{19}\text{Gev}$ . Although there are several proposals for the total unification of forces some of which invoke strings, M-theory, extra dimensions and a variety of novel and fascinating new concepts, the experimental confirmation of any of these ideas will not be available soon. However, the physics of the “standard” model of the strong and electroweak interactions that describes phenomena at energy scales below  $\sim 100\text{ Gev}$  is on solid experimental footing.

The connection between the standard model of particle physics and early Universe cosmology is through Einstein’s equations that couple the space-time geometry to the matter-energy content. We argued above that at energy scales well below the Planck scale gravity can be studied classically. However, the standard model of particle physics is a *quantum field theory*, thus the question arises: how to treat classical space-time but with sources that are quantum fields. The answer to this question is: semiclassically, Einstein’s equations (without the cosmological constant) are interpreted as

$$G^{\mu\nu} = R^{\mu\nu} - \frac{1}{2}g^{\mu\nu}R = \frac{8\pi}{M_{Pl}^2}\langle\hat{T}^{\mu\nu}\rangle \quad (2.14)$$

with  $\hat{T}^{\mu\nu}$  is the *operator* energy momentum tensor and the expectation value is taken in a given quantum state (or density matrix). A state that is compatible with homogeneity and isotropy must be translational (and rotational) invariant, and the expectation value of the energy momentum tensor operator must have the fluid form  $\langle T_{\nu}^{\mu}\rangle = \text{diag}[\rho, -p, -p, -p]$ .

Therefore, through this identification the standard model of particle physics provides the sources for Einstein’s equations. All of the elements are now in place to understand the evolution of the early Universe from the fundamental standard model. Einstein’s equations determine the evolution of the scale factor, the standard model provides the energy momentum tensor.

### 2.3 Energy scales:

While a detailed description of early Universe cosmology is available in many excellent books [3]-[7], a broad-brush picture of the main cosmological epochs can be obtained by focusing on the energy scales of particle, and atomic physics.

**Total Unification:** Gravitational, strong and electroweak interactions are conjectured to become unified and described by a single quantum theory at the Planck scale  $\sim 10^{19}\text{Gev}$ . While there are currently many proposals that seek to provide such fundamental description, these are still fairly speculative and no experimental confirmation is yet available.

**Grand Unification:** Strong and electroweak interactions (perhaps with supersymmetry) are conjectured to become unified at an energy scale  $\sim 10^{15}\text{ Gev}$  corresponding to a temperature  $T \sim 10^{28}\text{K}$ . There are very compelling theoretical reasons (such as the joining of the running coupling constants) that lead to this conjecture, but there is as yet no experimental evidence in favor of these ideas.

**Electroweak :** Weak and electromagnetic interactions become unified in the electroweak theory based on the gauge group  $SU(2) \otimes U(1)_Y$ . The weak interactions become short ranged after a symmetry breaking phase transition  $SU(2) \otimes U(1)_Y \rightarrow U(1)_{em}$  at an energy scale of the order of the mass of the  $Z_0, W^{\pm}$  vector bosons,  $E \sim 100\text{Gev}$  corresponding to a temperature  $T_{EW} \sim 100\text{ Gev}$ . At temperatures  $T > T_{EW}$  the symmetry is restored and all vector bosons are (almost) massless (save for plasma effects that induce screening masses). For  $T < T_{EW}$  the vector bosons that mediate the weak interactions (neutral and charged currents)  $W^{\pm}, Z_0$  acquire masses while the photon remains massless. Thus  $T_{EW}$  determines the temperature scale of the electroweak phase transition in the early Universe and is the *earliest* phase transition that is predicted by the standard model of particle physics.

**QCD:** The strong interactions have a typical energy scale  $\Lambda_{QCD} \sim 200\text{Mev}$  at which the coupling constant becomes of order one. This energy scale corresponds to a temperature scale  $T_{QCD} \sim 10^{12}\text{K}$ . QCD is an asymptotically free theory, the coupling between quarks and gluons becomes smaller at large energies, but it diverges at the scale  $\Lambda_{QCD}$ . For energy scales below  $\Lambda_{QCD}$  QCD is a strongly interacting theory. This phenomenon is interpreted in terms of a phase transition at an energy scale  $\Lambda_{QCD} \sim 200\text{ Mev}$  or  $T_{QCD} \sim 10^{12}\text{ K}$ . For  $T > T_{QCD}$  the relevant degrees of freedom are weakly interacting quarks and gluons, while below are hadrons. This is the quark-hadron or confinement-deconfinement phase transition. At about the same temperature scale QCD has another phase transition that results in chiral symmetry breaking (for more details see section 4). The QCD phase transition(s) are the *last* phase transition predicted by the standard model of particle physics. The high temperature phase above  $T_{QCD}$ , with almost free quarks and gluons (because the coupling is small by asymptotic freedom) is a *quark-gluon plasma* or QGP for short. Current experimental programs at CERN (SPS-LHC) and Brookhaven National Laboratory (AGS-RHIC) are studying the QCD phase transition via ultrarelativistic heavy ion collisions and a systematic analysis of the data gathered at SPS-CERN during the last decade has given an optimistic perspective of the existence of the QGP [34, 35] (see section 4 below).

**Nuclear Physics:** Low energy scales that are relevant for cosmology are determined by the binding energy of light elements, in particular deuterium, whose binding energy is  $\sim 2\text{ Mev}$  corresponding to a temperature  $T_{NS} \sim 10^{10}\text{ K}$ . This is the energy scale that determines the onset of primordial nucleosynthesis, as described below.

**Atomic Physics:** Another very important low energy scale relevant for cosmology corresponds to the binding energy of hydrogen  $\sim 10\text{ eV}$ . This is the energy scale at which free protons and electrons combine into neutral hydrogen. As it will be described below the relevant scale is more like  $\leq 0.3\text{ eV}$  corresponding to a temperature  $T \sim 3 \times 10^3\text{ K}$ .

Based on the ingredients described above, a very detailed picture of the thermal history of the Universe emerges [3]-[7]: during the first  $\sim 10000$  years after the Big Bang the Universe was radiation dominated expanding and cooling (almost) adiabatically. As a consequence the entropy  $S \propto V(t)T^3(t) \propto V_0 [a(t)T(t)]^3$  is constant, implying  $T = T_0/a(t)$ . Radiation domination, in turn, results in that  $a(t) \propto t^{\frac{1}{2}}$  and a detailed analysis [3]-[7] reveals that

$$T(t) \sim \frac{10^{10}\text{K}}{t^{\frac{1}{2}}(\text{sec})} \sim \frac{1\text{ Mev}}{t^{\frac{1}{2}}(\text{sec})} \quad (2.15)$$

## 3 Phase Transitions and their aftermath

### 3.1 GUT's and inflation

Current theoretical ideas of theories beyond the standard model suggest that there could have been a phase transition at the GUT scale  $T_{GUT} \sim 10^{15}\text{ Gev} \sim 10^{32}\text{ K}$ . This energy scale is also usually associated with an important cosmological stage: inflation, during which the acceleration of the scale factor is *positive* which implies via eqn. (2.9) that  $p < -\rho/3$ . Inflation plays a very important role in early Universe cosmology and current observations of the power spectrum of temperature anisotropies seem to confirm the robust features of the inflationary proposal [1]. While I will not attempt to review all features of inflationary cosmology, for which the reader is referred to the literature [3]-[7], I summarize some of the most important concepts so as to make contact with the observable consequences of phase transitions later.

As is mentioned above, inflation corresponds to an epoch of accelerated expansion, i.e, with  $\ddot{a}(t) > 0$  which from eqn. (2.9) requires that  $p < -\rho/3$ . Within particle physics models this is achieved by considering the energy momentum tensor of a scalar field, which in principle is one of the fields in the GUT. For a scalar field the energy density and the pressure are given by [3]-[7]

$$\rho = \frac{\dot{\varphi}^2}{2} + \frac{(\nabla\varphi)^2}{2a^2(t)} + V(\varphi) \quad (3.1)$$

$$p = \frac{\dot{\varphi}^2}{2} - \frac{(\nabla\varphi)^2}{2a^2(t)} - V(\varphi) \quad (3.2)$$

where  $V(\varphi)$  is the scalar potential.

Inflation results from the generalized slow-roll condition [3]-[7]

$$V(\varphi) \gg \dot{\varphi}^2, \quad \frac{(\nabla\varphi)^2}{a^2(t)} \quad (3.3)$$

which results in that  $\rho = -p \sim V(\varphi) \simeq \text{constant}$  leading to the De Sitter solution eqn.(2.13) for the scale factor. This situation can be achieved via a variety of inflationary scenarios (old, new, chaotic, hybrid etc.) [3]-[7]. With the purpose of establishing contact with observational consequences of phase transitions I focus the discussion on either a first order (old inflation) or second order (new inflation) phase transition [3]-[7] at the GUT scale.

In these situations the expectation value of the scalar field is at a false vacuum extremum of the potential with a very slow time evolution. The expansion of the Universe red-shifts the inhomogeneities of the field and the slow-roll condition (3.3) is fulfilled. In these scenarios the expectation value of the scalar field is nearly constant during the inflationary stage leading to a De Sitter expansion of the scale factor as in eqn. (2.13) with

$$H = \sqrt{\frac{8\pi V(\varphi)}{3M_{Pl}^2}} \quad (3.4)$$

Inflation terminates when the field “rolls down” to the minimum of potential, where further oscillations result in particle production, reheating and a transition to a standard hot big bang, radiation dominated era [3]-[7]. While the evolution of the scale factor along with the dynamics of the scalar field (inflaton) were typically studied using the *classical* equations of motion for the scalar field, more recently a consistent description of the *quantum dynamics* has been provided [8, 9, 12]. The non-equilibrium dynamics of cosmological phase transitions requires a non-perturbative framework that treats self-consistently the dynamics of the matter field and the evolution of the metric. This framework leads to a detailed understanding of the classicalization of quantum fluctuations as well as to a microscopic justification for inflation in a full quantum field theory. We refer the reader to ref. [8, 9, 12] for more details which fall outside the main scope of these lectures.

An important aspect of inflationary dynamics and one that is very relevant to the discussion of observables associated with phase transitions stems from the positive acceleration of the scale factor. A simple calculation shows that

$$\frac{\ddot{a}(t)}{a(t)} > 0 \implies \frac{\dot{a}(t)}{a(t)} > \frac{\dot{d}_H(t)}{d_H(t)} \quad (3.5)$$

Therefore during a period of accelerated expansion or inflation, *the scale factor grows faster than the Hubble radius*. In particular for De Sitter inflation while the Hubble radius  $d_H = 1/H$  is constant, the scale factor grows exponentially  $a(t) = a_0 e^{Ht}$ . This feature of accelerated expansion is indeed remarkable. Consider a perturbation of physical wavelength  $\lambda_{phys}(t) = \lambda_c a(t)$  where  $\lambda_c$  is the comoving wavelength. When  $\lambda_{phys}(t) < d_H$  causal microphysical processes can affect this perturbation, but when this wavelength “crosses the horizon” i.e, when  $\lambda_{phys}(t) > d_H$  no causal process can affect the perturbation. Thus physical

wavelengths *inside* the Hubble radius (or loosely speaking the causal horizon) are causally connected and influenced by microphysical processes. When these wavelengths cross the horizon they stretch *superluminally* and “decouple” from causal processes, hence their evolution is not affected by microphysical processes.

We note that for matter or radiation dominated cosmologies  $a(t) \propto t^{2/3}$ ,  $t^{1/2}$  respectively, for which the Hubble radius  $d_H(t) = 3t/2$ ,  $2t$  respectively, grows *faster* than the scale factor. Therefore wavelengths that at some time are outside the Hubble radius, eventually “cross the horizon” back inside the Hubble radius.

Since inflation is followed by the standard hot big bang cosmology with a radiation and matter dominated eras, physical wavelengths that are *inside* the Hubble radius during inflation, and cross *outside* during inflation will re-enter during the radiation or matter dominated eras. This situation is depicted in figure (1) below.

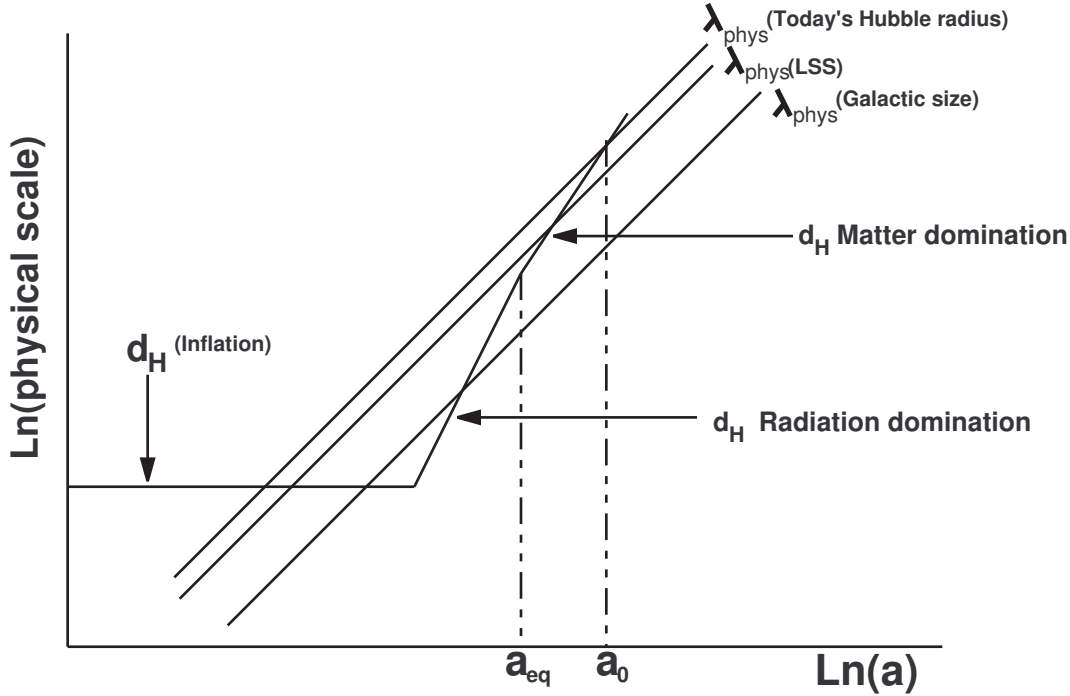


Figure 1: Logarithm of physical scales vs. logarithm of the scale factor. The causal horizon  $d_H$  is shown for the inflationary (De Sitter), radiation dominated and matter dominated stages. The physical wavelengths ( $\lambda_{phys}$ ) for today’s Hubble radius, the surface of last scattering (LSS) and a galactic scale are shown.  $a_{eq}$ ,  $a_0$  refer to the scale factor at matter-radiation equality and today, respectively.

The wavelengths that are of cosmological relevance *today* say with  $1 \text{ Mpc} \lesssim \lambda_{phys}(t_0) \lesssim 3000 \text{ Mpc}$  crossed the horizon during the last  $\sim 10$  e – folds of inflation[3].

### 3.1.1 Density perturbations and the signature of a phase transition

This important feature of accelerated expansion and inflation, i.e., that physical wavelengths within the causal horizon during inflation cross-out and re-enter during radiation or matter domination, provides the mechanism for “seeding” temperature anisotropies. Inflation “seeds” temperature inhomogeneities in the cosmic microwave background and the matter density inhomogeneities that lead to large scale structure



formation from primordial quantum fluctuations whose wavelengths were inside the Hubble radius during inflation [3]-[7].

To see this more clearly, consider small amplitude perturbations of the homogeneous scalar field that drive inflation

$$\varphi(\vec{x}, t) = \varphi(t) + \delta\varphi(\vec{x}, t) \quad (3.6)$$

This perturbation induces a small perturbation in the energy density, which to linear order in  $\delta\varphi(\vec{x}, t)$  and taking the spatial Fourier transform is [3]-[7]

$$\delta_{\vec{k}} = \frac{\delta\rho_{\vec{k}}}{\rho} \propto \delta\varphi_{\vec{k}} \quad (3.7)$$

The power spectrum of density perturbations is obtained from the quantum average

$$\langle |\delta_{\vec{k}}|^2 \rangle \propto \langle |\delta\varphi_{\vec{k}}|^2 \rangle. \quad (3.8)$$

An important and robust result from inflation is that [3]-[7]

$$\langle |\delta_{\vec{k}}|^2 \rangle \propto k^{n_s - 1}; \text{ with } n_s \sim 1 \quad (3.9)$$

This power law spectrum with  $n_s \sim 1$  is (almost) scale invariant and referred to as Harrison-Zeldovich. As it will be discussed in the section on the CMB below, this power spectrum is measurable through the temperature anisotropies at the surface of last scattering [6, 3].

The main point of this discussion is that inflation generates temperature anisotropies and density perturbations from *quantum fluctuations* whose wavelengths cross the horizon during inflation and re-enter just before recombination [3, 5, 6] (see fig. 1).

Phase transitions during inflation modify the power spectrum of the quantum fluctuations. After the wavelength of these fluctuations crosses the horizon during inflation, they evolve acausally carrying with them the information of the phase transition without being affected by microphysical processes. When the wavelengths of these fluctuations re-enter the horizon near recombination the information of the phase transition is imprinted in the temperature anisotropies in the CMB through departures from scale invariance in the power spectrum (3.8), i.e,  $n_s \neq 1$  as a consequence of the phase transition.

To illustrate these ideas in a simple setting, let us consider a simple scalar field theory with the potential

$$V(\varphi) = \frac{\lambda}{4} \left( \varphi^2 - \frac{m^2}{\lambda} \right)^2 \quad (3.10)$$

This is the typical potential that leads to (a second order) phase transition. The strength of the self-coupling  $\lambda$  is constrained by the amplitude of the temperature anisotropies to be [5]  $\lambda \sim 10^{-12}$ . During the phase transition, the expectation value of the scalar field  $\varphi \sim 0$ . Requiring that the energy density is given by the GUT scale

$$\rho \sim \frac{m^4}{4\lambda} \sim (10^{15} \text{ GeV})^4$$

during the epoch of the phase transition determines that  $m \sim 10^{12}$  GeV. The Hubble constant is then given during this stage by

$$H^2 \approx \frac{2\pi}{3} \frac{m^4}{\lambda M_{Pl}^2} \implies \frac{H}{m} \sim \mathcal{O}(1) \quad (3.11)$$

Therefore during the phase transition when  $\varphi \sim 0$  the expansion is of De Sitter type and small amplitude fluctuations of the scalar field (in terms of the spatial Fourier transform)  $\delta\varphi_{\vec{k}}$  obey the linearized equation

$$\ddot{\delta\varphi_{\vec{k}}}(t) + 3H\dot{\delta\varphi_{\vec{k}}}(t) + \left[ \frac{\vec{k}^2}{a^2(t)} - m^2 \right] \delta\varphi_{\vec{k}}(t) = 0. \quad (3.12)$$

We note that the sign of the mass squared term is negative as required to describe a symmetry breaking phase transition. Setting  $H = 0$ ,  $a = 1$ , i.e. in Minkowsky space time we recognize that long-wavelength fluctuations with  $k^2 < m^2$  grow exponentially. These are the *spinodal instabilities*, a hallmark of the process of phase separation during the phase transition [10, 12]. During the stage of De Sitter inflation, eqn.(3.12) has the following solution [9]

$$\begin{aligned} \delta\varphi_{\vec{k}}(t) &= e^{-\frac{3Ht}{2}} \left[ A_k J_\nu \left( \frac{k}{H} e^{-Ht} \right) + B_k J_{-\nu} \left( \frac{k}{H} e^{-Ht} \right) \right] \\ \nu &= \sqrt{\frac{9}{4} + \frac{m^2}{H^2}} \end{aligned} \quad (3.13)$$

the coefficients  $A_k, B_k$  are determined by initial conditions[9]. When the physical wavevector crosses the horizon, i.e. when  $k e^{-Ht} \ll H$  the solution grows exponentially and is given by

$$\delta\varphi_{\vec{k}}(t) \propto e^{(\nu - \frac{3}{2})Ht} \quad (3.14)$$

In the limit  $H \ll m$  this solution displays the spinodal long-wavelength instabilities  $\propto e^{mt}$  associated with the phase transition in Minkowski space-time [10, 12]. Thus the exponential growth of superhorizon fluctuations given by (3.14) is a direct consequence of the spinodal instabilities associated with the phase transition *during the De Sitter inflationary epoch*. A detailed calculation of the power spectrum of density fluctuations [9, 11] yields

$$\langle |\delta_{\vec{k}}|^2 \rangle \propto k^{-2(\nu - \frac{3}{2})} \Rightarrow n_s = 1 - 2(\nu - \frac{3}{2}) \quad (3.15)$$

since  $\nu > 3/2$  we see that there is more power at long wavelengths. This is obviously a consequence of the spinodal instabilities associated with the phase transition. Thus we arrive at an important result that provides an observational signal of the phase transition: *the power spectrum of density perturbations is tilted to the red, i.e. the index is smaller than one. This is because the spinodal instabilities associated with the phase transition imply larger amplitudes for longer wavelengths, thus enhancing the infrared*. After these perturbations re-enter the horizon close to recombination, this power spectrum is imprinted in the temperature anisotropies of the CMB (see the discussion on the CMB below) which are measured. The four year COBE-DMR Sky Map[13] gives  $n_s \sim 1.2 \pm 0.3$ , thus a (second order) phase transition at the GUT scale is consistent with this power spectrum if  $H/m \geq 3$  which, in turn, is consistent with GUT scale inflation as can be seen from eqn.(3.11).

This simple example thus provides a good idea of the potential observational signatures of phase transitions at the GUT scale associated with an inflationary era: a power spectrum with a red-tilt results if the phase transition is triggered by spinodal instabilities during the inflationary epoch.

Another potential observable from an inflationary phase transition was proposed recently [14]. These authors pointed out that the breaking of scale invariance in the primordial power spectrum by an inflationary phase transition could lead to a step-like spectral feature, which seems to be compatible with recent measurements of the CMB and large scale surveys (APM).

Thus observations of the temperature anisotropies in the CMB could provide information on inflationary phase transitions. Furthermore, a “reconstruction” program seeks to extract some aspects of the scalar potential from the CMB temperature anisotropies [15], therefore providing a further link between phase transitions during the inflationary era and the temperature anisotropies of the CMB.

### 3.2 The Electroweak Phase Transition: Baryogenesis?

The EWPT is the *first* symmetry breaking phase transition predicted by the standard model of particle physics. It occurred at a temperature  $T_{EW} \sim 100 \text{ GeV} \sim 10^{15} \text{ K}$  at about  $t \sim 10^{-12}$  secs after the Big Bang when the Hubble radius was  $d_H \sim 10^{-1} \text{ cm}$ . The symmetry breaking pattern is  $SU(2) \otimes U(1)_Y \rightarrow U(1)_{em}$ . Probably the most tantalizing observable from the electroweak phase transition *could be the baryon asymmetry*. There is an asymmetry between particles and antiparticles in the observed Universe, large regions of antimatter would result in particle annihilations leading to a diffuse  $\gamma$ -ray background and distortions of the CMB. None of which is observed, leading to the conclusion that the Universe is made up of particles up to the Hubble radius [16]. Furthermore Big Bang nucleosynthesis provides accurate predictions for the abundance of light elements up to  ${}^7\text{Li}$  in terms of the ratio of the baryon density to the photon density

$$\eta = \frac{n_b - \bar{n}_b}{n_\gamma} \quad (3.16)$$

Observations of the abundance of light elements constrain this parameter to be in the range [3]

$$4 \times 10^{-10} \lesssim \eta \lesssim 7 \times 10^{-10} \quad (3.17)$$

The important question is: what is the origin of the baryon asymmetry (baryogenesis)? (for a recent review on baryogenesis see [16]).

The necessary conditions required for baryogenesis were identified originally by Sakharov [17]

- C and CP violation
- Baryon number violation
- Departure from thermal equilibrium

The EW theory violates maximally P (parity) and also C (charge conjugation). CP violation is observed in the  $K^0, \bar{K}^0$  system (and currently also in the  $B^0, \bar{B}^0$  system) and is experimentally determined by the parameters  $\epsilon \sim 2.3 \times 10^{-3}$ ,  $\epsilon' \sim 5.2 \times 10^{-6}$  that measure indirect (through mixing of eigenstates) and direct CP violation. CP violation in the standard model is a consequence of the phase in the CKM mass matrix for three generations.

Baryon number violation in the EW theory is a consequence of non-perturbative gauge (and Higgs) field configurations that interpolate between topologically different vacua. A transition between two adjacent vacua leads to one unit of baryon number violation per family (for details see [16]). While at zero temperature this is a vacuum tunneling process which is suppressed by the barrier penetration factor  $e^{-\frac{2\pi}{\alpha_w}}$  with  $\alpha_w \sim 1/30$ , at finite temperature the transition is overbarrier, i.e, thermal activation. The overbarrier transitions are unsuppressed at temperatures of the order of  $T_{EW}$  [16].

The requirements of baryon number violation and CP violation are clear: to generate any asymmetry the theory must allow for processes that produce the quantum number in question (B) and to also distinguish particle from antiparticle (CP). If the relevant processes are in equilibrium then the rate for particles and that

of antiparticles are related by detailed balance and since CPT invariance implies that the masses of particles are equal to those of antiparticles, the distribution functions for both are identical and no asymmetry can result [3, 16].

The expansion of the Universe alone cannot provide the non-equilibrium ingredient. To see this let us compare the reaction rate of weak interactions (the electromagnetic interactions are much faster than the weak interactions) to the expansion rate of the Universe. Since the EWPT takes place during a radiation dominated era with  $\rho \propto T^4$  the expansion rate is given by

$$H \propto \frac{T^2}{M_{Pl}} \quad (3.18)$$

The reaction rate is given by  $\Gamma = n\sigma_w$  with  $n$  the particle density and  $\sigma_w$  the cross section. The typical weak interaction cross section is  $\sigma_w \sim G_F^2 E^2$  with  $G_F \sim 10^{-5}/\text{Gev}^2$ , at temperature  $T$  the typical energy is  $E \sim T$  and a particle density  $n \sim T^3$ . Thus the weak interaction rate  $\Gamma = n\sigma_w$  is of order

$$\Gamma \sim G_F^2 T^5 \quad (3.19)$$

therefore the ratio

$$\frac{\Gamma}{H} \sim G_F^2 M_{Pl} T^3 \sim [10^3 T(\text{Gev})]^3 \quad (3.20)$$

determines whether the weak interactions are in local thermal equilibrium (LTE). At  $T \sim T_{EW}$  the ratio is  $\Gamma/H \sim 10^{15}$ , therefore weak interaction processes are in LTE (and obviously electromagnetic processes will be more so).

Instead departures from equilibrium results from a *strong* first order phase transition that occurs via the nucleation of bubbles of the true phase in a background of the metastable phase [16].

Detailed numerical simulations of the EWPT[18] reveal that it is first order if the Higgs mass  $M_H < 80\text{Gev}$  but above this value it is a smooth crossover. Recently, however, a summary of all the data collected by the four detectors at LEP up to energy 202 Gev, seem to indicate that the Higgs has a mass  $M_H \gtrsim 115\text{Gev}$ [19]. Thus it is very likely that the (minimal) standard model cannot accomodate a strong first order phase transition that will produce the non-equilibrium conditions sufficient for baryogenesis. Furthermore, it is now clear that the CP violation in the (minimal) standard model, encoded in the parameters  $\epsilon, \epsilon'$  (or alternative in the phase of the CKM matrix) is too small to explain the observed baryon asymmetry.

Thus, the current theoretical understanding seems to suggest that the baryon asymmetry cannot be explained by the minimal standard model although the Minimal Supersymmetric Standard Model (MSSM) may accomodate all of the necessary ingredients [16]. Hence the cosmological consequences of the EWPT are not very clear. Furthermore, while accelerator experiments (Tevatron and LHC) will probably lead to an assessment of the Higgs mass and CP violating parameters, a *direct* study of the EWPT will not be feasible soon. Indeed in order to study it an energy *density* of order  $\rho_{EW} \sim T_{EW}^4$  must be achieved, but with  $T_{EW} \sim 100 \text{ Gev}$  this energy density is  $\rho_{EW} \sim 10^{11} \rho_n$  where  $\rho_n \sim 0.15 \text{ Gev}/\text{fm}^3$  is the energy density of nuclear matter!!.

### 3.3 The QCD phase transition(s)

The next and *last* phase transition predicted by the standard model of particle physics takes place at the QCD scale  $T \sim 100 - 200\text{Mev}$ . It occurred when the Universe was about  $t \sim 10^{-5} - 10^{-6}$  seconds old and the Hubble radius was  $d_H \sim 10\text{Km}$ . QCD is an asymptotically free theory, that is the gauge coupling constant between quarks and gluons varies with energy through “vacuum polarization” effects as

$$\alpha_s(E) = \frac{4\pi}{(11 - \frac{2}{3}N_f) \ln \left[ \frac{E^2}{\Lambda_{QCD}^2} \right]} ; \quad \Lambda_{QCD} \sim 200 \text{Mev} ; \quad \alpha_s = \frac{g^2}{4\pi} \quad (3.21)$$

with  $N_f$  being the number of flavors and  $g$  is the quark-gluon coupling. For  $E \gg \Lambda_{QCD}$  quarks and gluons are weakly coupled, but for  $E \sim \Lambda_{QCD}$  the coupling becomes strong, diverging at  $E = \Lambda_{QCD}$ . This divergence is interpreted as a transition between a state of almost free quarks and gluons to a state in which quarks and gluons are confined inside hadrons. This is the *confinement-deconfinement transition* and the QCD scale  $\Lambda_{QCD}$  determines the range of temperature for this transition. The high temperature phase in which quarks and gluons are almost free is referred to as the *Quark Gluon Plasma* or QGP for short.

Because the up and down quark masses are so much smaller than  $\Lambda_{QCD}$  ( $m_u \sim 5 \text{ Mev}$ ;  $m_d \sim 10 \text{ Mev}$ ) the low energy sector of QCD has an  $SU(2)_R \otimes SU(2)_L$  symmetry in the limit of massless up and down quarks. This chiral symmetry corresponds to independent chiral rotations of the right and left handed components of the quark fields. However the ground state of QCD spontaneously breaks this chiral symmetry down to  $SU(2)_{L+R}$  leading to three massless Goldstone bosons. The small (and different) masses of the up and down quark provide a small explicit symmetry breaking term in the Lagrangian and as a consequence the (would be) Goldstone bosons acquire a mass. This triplet of almost Goldstone bosons are the neutral and charged pions, which are the lightest pseudoscalar particles with  $m_\pi \sim 140 \text{ Mev}$ . Lattice simulations [20] suggest that the confinement-deconfinement and chiral phase transitions occur at about the same temperature  $T \sim 160 \text{ Mev}$  (for a review see [21]). At this temperature only the lightest quark flavors influence the thermodynamics, the up, down and strange quarks with  $m_s \sim 150 \text{ Mev}$ . The chiral phase transition associated with the two lightest quark flavors is second order for massless quarks but either slightly first order or a crossover when the mass of the up and down quarks is accounted for, and is in the universality class of the  $O(4)$  Heisenberg ferromagnet. Including the strange quark the situation is more complicated and depends on whether the strange quark can be considered heavy or light, the transition becomes first order if the strange quark is light [20]. The complication arises because  $m_s \sim \Lambda_{QCD}$  and is therefore neither light nor heavy on the QCD scale.

The confinement-deconfinement transition for three flavors is likely to be of first order [20, 21] and therefore occurs via the nucleation of hadronic bubbles in the background of a QGP. An estimate of whether the expansion of the Universe at the QCD phase transition results in non-equilibrium effects can be obtained in the same manner as in the case of the EW transition, i.e, by estimating the ratio  $\Gamma/H$  with  $\Gamma$  a typical strong interaction reaction rate. A typical cross section is  $\sigma \sim 0.1 - 1 \text{ fm}^2$  and the number of particles at  $T_{QCD} \sim 200 \text{ Mev}$  is  $n \sim T_{QCD}^3 \sim 1/\text{fm}^3$  this leads to  $\Gamma \sim 1/\text{fm}/c \sim 10^{22} \text{ sec}^{-1}$  and since  $H \sim 10^6 \text{ sec}^{-1}$ , therefore  $\Gamma/H \sim 10^{16}$  and again the QGP is in LTE (local thermal equilibrium). However, just as in the case of the EWPT, non-equilibrium effects may arise from a first order phase transition through supercooling and the nucleation of bubbles. In this case, hadronic bubbles nucleate in the host of the QGP releasing latent heat. After a short period of reheating, the transformation between the QGP and the hadronic phases occurs in LTE until all of the QGP transforms into hadrons. Most of the hadrons decay on short time scales, for example charged pions decay on time scales  $\sim 10^{-8}$  secs, and neutral pions on much shorter time scale  $10^{-16}$  secs. Therefore most hadrons have decayed after a few  $\mu\text{secs}$  after the QCD PT but for neutrons, with a lifetime  $\sim 900$  secs and protons (with a lower limit for the lifetime of  $\sim 10^{32}$  years).

Since the QCD PT is the last phase transition, there is an important effort to understand its potential cosmological consequences. While the details are complex, not completely understood and cannot be given in this short review, the following important consequences are possible (for a recent review see also [22, 23])

- **Baryon inhomogeneities affect nucleosynthesis:** [24] The nucleation of hadronic bubbles in a host of QGP can lead to inhomogeneities in the baryon number density, with the scale for inhomogeneity determined by the typical distance between bubbles. These inhomogeneities may result in inhomogeneous neutron to proton ratios which in turn can lead to inhomogeneous nucleosynthesis (see the section on nucleosynthesis below) and modify the abundance of light elements. For the inhomogeneities

produced by bubble nucleation to modify the neutron to proton ratio for nucleosynthesis it must be that the typical separation between nucleating bubbles must be much larger than the proton and neutron diffusion lengths. Proton and neutrons have *different* diffusion lengths because of the Coulomb scattering of protons. An important criterion for inhomogeneous nucleosynthesis is that the mean scale for baryon inhomogeneity at the time of the QCD PT, i.e, the mean distance between nucleating bubbles must be of order  $\sim 1$  meter [24]. This distance depends on the latent heat released during the (first order) phase transition, the free energy difference between the QGP and the hadron gas phases and the surface tension for the nucleating bubble. More recent analysis [25] seems to point out that the distance between bubbles produced during homogeneous nucleation is  $d_{nuc} \sim 1\text{cm}$ . Larger values of  $d_{nucl}$  can arise from inhomogeneous nucleation seeded by “impurities” [25]. These inhomogeneities can be produced by primordial black holes (see below) as proposed by [25] or by primordial density fluctuations as suggested by [26].

However as recognized in the literature [24, 25, 26] much more needs to be understood about the phase structure of QCD before a quantitatively reliable statement can be made. Of particular importance are details of the equation of state (EoS), surface tension, which determines the size of the nucleating bubbles, and also the (in medium) mass of the strange quark. For a more recent estimate on inhomogeneous nucleosynthesis arising from a first order QCD PT see [27, 23].

- **Primordial Black Holes:** [28, 29] An important aspect of a first order phase transition (with only one globally conserved quantity, such as baryon number) is that during the coexistence or mixed phase of QGP and hadron gas, the Gibbs construction determines that the phase transition occurs at constant pressure (as well as temperature). If the pressure is constant, then the (adiabatic) speed of sound vanishes and there are no restoring pressure waves. This in turn means that there is no restoring force to counterbalance the gravitational collapse and long-wavelength density perturbations will grow under self-gravity causing the gravitational collapse of the mass contained in a volume of radius given by this wavelength. This observation leads to the possibility of formation of *primordial black holes* [28](for a discussion of gravitational collapse and Jeans instability see section 3.6). An important question is what is the mass of the black hole?, to obtain a qualitative estimate we can calculate the mass in the Hubble radius at the time of the QCD PT:  $M_H = 4\pi\rho d_H^3/3$  with  $d_H \sim 10\text{Km}$  the Hubble radius at the time of the PT. Using that  $H^2 = 1/d_H^2 = 8\pi\rho /3M_{Pl}^2$  therefore  $M_H = M_{Pl}^2 d_H/2 \sim 10^{57}\text{Gev} \sim 1M_\odot$ . Thus this order-of-magnitude estimate suggests that primordial black holes with mass up to  $\sim 1M_\odot$  may form during the QCD PT [28]. It is important to mention at this stage, that the Hubble radius at the QCD PT  $\sim 10^4 m$  extrapolated to today is  $\sim 0.2 \text{ pc}$  which is *much smaller* than the Hubble radius today  $\sim 3000 \text{ Mpc}$ . Therefore a large number of primordial black holes produced during the QCD PT would be present today.

A more detailed analysis of the possibility of primordial black hole formation and the ensuing density fluctuations has been provided recently [29]. The results of this reference, based on approximate or lattice EoS seem to lead to a less likely scenario for solar mass primordial black hole formation, but to an enhancement in the clumping of cold dark matter (CDM). It is fair to say, however, that there are still large uncertainties in the EoS and the relevant quantities that enter in the calculation. The experimental programs that seek to study the QGP in heavy ion colliders that are described below will lead to a more reliable understanding of the relevant aspects of the PT, EoS and QCD parameters. For more detailed aspects of primordial black holes, see [30].

- **Strange Quark Nuggets:** [31] Witten suggested that during a first order QCD PT in the early Universe a large amount of strange matter could be produced [32]. He also argued that strange matter could be absolutely stable with an energy per baryon which is less than the maximum binding energy (of Fe) 930MeV. While this scenario has been criticized (see Applegate and Hogan in [24]), the uncertainties in the knowledge of the QCD EoS, the (in medium) strange quark mass and other relevant QCD parameters leave enough room for the possibility of formation of strange quark “nuggets” [31]. Some of the consequences of the formation of strange quark nuggets during the (first order) QCD PT

had been investigated in [31, 33]. These strange nuggets can be part of the cold dark matter, and if they do not evaporate during  $\sim 1$  sec after the QCD PT, their presence can affect nucleosynthesis by modifying the neutron to proton ratio, thus modifying the  ${}^4\text{He}$  (and heavier elements) abundance [31].

The different possible signatures of the QCD PT in the early Universe as described by the scenarios above rely on the particular details of the phase transition as well as thermodynamic parameters that cannot be calculated in perturbation theory. Lattice gauge theory provides a non-perturbative approach to studying many of these aspects and although progress has been made in the field [20] the complications associated with light quarks beyond the quenched approximation still need further understanding. It is clear that probably the best assessment of the QCD phase diagram would be obtained from experiments that can probe the hot and dense phase(s) of QCD.

The heavy ion programs at the CERN-SPS and the BNL-AGS, and the current program at BNL-RHIC have as major goals to reveal the new state of matter described by the QGP. Almost two decades of experiments at CERN and BNL have provided a wealth of data that together reveal that this new state of matter, predicted by QCD may have been formed in ultrarelativistic heavy ion collisions. The recent announcements from CERN [34, 35] yield convincing arguments that there is already experimental evidence for the QGP. Thus there is the very tantalizing possibility that the next generation of ultrarelativistic heavy ion collisions at RHIC and eventually the ALICE (A Large Ion Collider Experiment) program at LHC will provide a more detailed understanding of the QCD PT, and from that data we can learn about the observable consequences of the same PT in the early Universe. This program, along with a brief summary of the recent results will be described in more detail in section 4.

### 3.4 Nucleosynthesis

The next stage down the ladder of energy scales corresponds to  $\sim 1$  Mev. This is the scale of binding energy of deuterium and determines the onset of primordial nucleosynthesis. As mentioned in the previous section, after the QCD confinement-deconfinement phase transition, the thermodynamics is described by a hadron gas. After about a  $\mu\text{sec}$  after this PT most hadrons decay and only neutrons and protons remain. Therefore the Universe can be characterized by a plasma of  $n, p, e^\pm, \nu's, \gamma's$ . Equation (3.20) for the ratio of a typical weak interaction reaction rate and the expansion rate of the Universe, determines that at a temperature  $T \sim 1$  Mev the weak interactions *freeze-out* (decouple), i.e, the rate for weak interaction processes is smaller than that of the expansion of the Universe. Eqn. (3.20) also means that the mean free path for the weak interactions is larger than the Hubble radius for  $T < 1$  Mev. A more detailed calculation [36] shows that the freeze-out or decoupling temperature is actually  $T_f = 0.8$  Mev. For  $T \gg T_f$  neutrons, protons, electrons and neutrinos are in nuclear statistical equilibrium via the weak interaction reactions

$$n \leftrightarrow p + e^- + \bar{\nu}_e ; \nu_e + n \leftrightarrow p + e^- ; e^+ + n \leftrightarrow p + \bar{\nu}_e \quad (3.22)$$

Since neutrons and protons are non-relativistic near the freeze-out temperature, their phase space distribution is determined by the usual Boltzmann distribution function and at any given temperature much smaller than their masses the neutron to proton ratio is given by

$$\frac{N_n}{N_p} = e^{-\frac{\Delta m}{T}} = e^{-\frac{1.29}{T(\text{Mev})}} \quad (3.23)$$

with  $\Delta m$  the neutron-proton mass difference. The neutron to proton ratio at  $T \sim T_f$  is given by

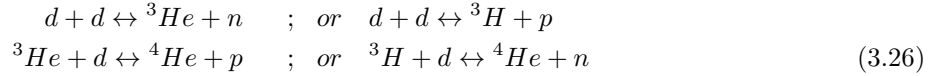
$$\frac{N_n}{N_p} = e^{-1.29/0.8} \sim 1/6 \quad (3.24)$$

After the Universe has cooled to the freeze-out temperature  $T_f$  this ratio remains fixed but for the decay of the neutron with a lifetime  $\sim 900$  secs.

Nucleosynthesis begins via the reaction



and continues through the following two possible paths towards the conversion of all neutrons into  ${}^4\text{He}$



The binding energy of deuterium is 2.22 Mev and *a priori* one would think that once the temperature falls below this value the reaction (3.25) will mainly go to the right. However, because the number of photons is so much larger than the number of baryons since  $n_B/n_\gamma \propto \eta$  with  $\eta$  given by eqn. (3.17) *there are too many photons in the high energy tail of the blackbody distribution* to photodisintegrate any deuterium formed until the temperature actually falls to  $T \sim 0.1$  Mev at a time of about 2 minutes [3]. This is the “deuterium bottleneck”: nucleosynthesis does not begin in earnest until the first step (3.25) happens. The formation of deuterium is hindered by the fact that the Saha equation for the equilibrium abundance for a species of atomic number A, contains a factor  $\propto \eta^{A-1}$  [3]. From the time of freeze-out when the temperature was  $T \sim T_f$  until deuterium is formed, the neutrons have decayed via the weak interactions (with a lifetime  $\sim 900$  secs) to a neutron to proton ratio  $N_n/N_p \sim 1/7$  [3, 36]. As soon as deuterium is formed the second stage(s) (3.26) occur fairly fast [3, 36] and all neutrons are used up in the formation of  ${}^4\text{He}$ . The neutron to proton ratio determines the abundance of  ${}^4\text{He}$ : each atom of  ${}^4\text{He}$  has two protons and two neutrons, but for each two neutrons 14 protons are needed because of the ratio 1/7. Altogether there are 16 baryons, out of which one Helium atom was formed, so the abundance of Helium is 25%! A network of nuclear reactions leads to the formation of light elements up to  ${}^7\text{Li}$  [36]. However because there is no nucleus with  $A = 5$  and no stable one with  $A = 8$  with unstable nuclei in between ( ${}^6\text{Li}, {}^7\text{Be}$ ) only small quantities of light elements other than  ${}^4\text{He}$  are produced. An important ingredient in these calculations, besides the nuclear cross sections that determine the nuclear reaction rates that have been measured in low energy experiments is the baryon to entropy ratio  $\eta$  which in turn can be related simply to  $\Omega_b h^2$  where  $\Omega_b$  is the ratio of the baryon density to the critical density [3, 36]  $\Omega_b h^2 \sim 3.64 \times 10^7 \eta$ .

Big Bang nucleosynthesis provides a precise estimate of the baryon density of the Universe by comparing to observations of the abundance of deuterium. The most recent observations [37] constrain the baryon density inferred from *standard* big bang nucleosynthesis to the interval

$$0.015 \lesssim \Omega_b h^2 \lesssim 0.024 \quad (3.27)$$

with  $\Omega_b$  being the baryon density expressed as a fraction of the critical density and  $h$  has been introduced in eqn. (2.2). In the past year, however, combined results on the CMB anisotropies from the balloon experiments BOOMERANG and MAXIMA and observations from type Ia supernovae have set new limits for the baryon density [38] (independent from the observation of abundances)

$$0.022 \lesssim \Omega_b h^2 \lesssim 0.039 \quad (3.28)$$

Although these results may be preliminary and require other observations for definite confirmation, taken together they signal the possibility of non-standard nucleosynthesis. These new observational constraints on  $\Omega_b$  have rekindled the interest on the possibility of inhomogeneous nucleosynthesis [27] with encouraging results for the abundances of deuterium and helium but the abundance predicted by these models of inhomogeneous nucleosynthesis for heavier metals is still well below the observed values.

The important point in this discussion and the main reason for delving into the subject of nucleosynthesis is to highlight two important factors that can be influenced by the QCD phase transition: i) the helium



abundance depends crucially on the neutron to proton ratio, although it is only slightly sensitive to the baryon to photon ratio. ii) The abundance of heavier elements up to  ${}^7\text{Li}$  depends in an important manner on the baryon to photon ratio. The point being made here is that if the QCD phase transition is of first order, there is the potential for producing inhomogeneities that modify the neutron to proton ratio, hence the helium abundance, as well as the baryon to photon ratio, and therefore the abundance of heavier elements. Hence if the value of  $\Omega_b h^2$  favored by BOOMERANG-MAXIMA and Type Ia supernovae searches stand up to further and deeper scrutiny, and are still in discrepancy with standard big bang nucleosynthesis perhaps inhomogeneous nucleosynthesis at the QCD phase transition could provide an explanation or be a part of the explanation.

### 3.5 Recombination, LSS and CMB

Continuing down the ladder of energy scales, the next step corresponds to energies of order eV determined by the binding energy of the hydrogen atom. Actually two different (but related) processes occur at this energy scale: a) (re) combination of electrons and protons into neutral hydrogen atoms which is described by the chemical reaction



b) photon decoupling (or freeze out): electrons and photons are in LTE through Thompson scattering  $e^- + \gamma \rightarrow e^- + \gamma$ . This electromagnetic process has the (large) cross section

$$\sigma_T = \frac{8\pi\alpha^2}{3m_e^2} = 6.6 \times 10^{-25} \text{cm}^2 \quad (3.30)$$

When the reaction rate  $\Gamma_\gamma = n_e\sigma_T$  with  $n_e$  the electron density becomes smaller than the expansion rate (or alternatively the photon mean free path becomes larger than the Hubble radius) the photons do not scatter any more, their distribution freezes and redshifts with the expansion. When the free electrons combine with protons binding into neutral hydrogen atoms the reaction rate becomes very small. Detailed calculations [3] reveal that recombination and decoupling occur at a temperature  $T_R \sim 3000\text{K}$  at a redshift  $z \sim 1100$ . The reason that the recombination temperature is *not* given by the binding energy of the hydrogen atom (= 13.6 eV) is again a consequence of the fact that the baryon to photon ratio is so small as given by (3.17) that even a small number of energetic photons in the blackbody tail can photodisintegrate the hydrogen atoms formed at  $T > T_R$ .

The important point here is that at a redshift  $z \sim 1100$  and temperature  $T_R \sim 3000\text{K}$  photons freeze-out, i.e. they do not undergo any further scattering. This occurs at a time  $t_R \sim 300000$  years after the Big Bang which defines the Last Scattering Surface (LSS). Photons have been travelling to us from the last scattering surface without scattering for the last  $\sim 15$  billion years and carry information of the LSS.

The discovery of the temperature anisotropies in the CMB by the COBE satellite with  $\Delta T/T \sim 10^{-5}$  on angular scales from  $90^\circ$  down to about  $2^\circ$  raises *two* fundamental questions:

- **The Horizon Problem:** photon decoupling occurs at  $t \sim 300000$  years after the Big Bang at a redshift of  $z \sim 1100$ . At this time the Hubble radius is  $d_H(t_R) \sim 100$  Kpc which determines the size of a correlated region. *Today* the size of this correlated patch is  $\sim (1+z)d_H(t_R) \sim 100$  Mpc, however the Hubble radius today is  $\sim 3000$  Mpc. Therefore we would expect that in the Hubble volume today there are about  $\sim 30000$  of these regions. Inside each of these regions the temperature fluctuations would be correlated but the regions would be completely uncorrelated between them. Each correlated patch today subtends an angle of about  $2^\circ$  which is the angular scale of the LSS today. However the CMB is homogeneous to 1 part in  $10^5$  on angular scales between  $2^\circ$  up to  $90^\circ$  as revealed by COBE. Thus the question: how did these regions that were outside the causal horizon of each other at photon decoupling manage to establish correlations and be so homogeneous in temperature?.

- **The origin of the temperature anisotropies:** what “seeds” the temperature inhomogeneities?. Simple statistical fluctuations are far too small. This can be seen by considering the simple case of a lump of matter with about one solar mass which has about  $10^{57}$  particles. Statistical fluctuations will be of order  $\sim 10^{-23}$  which cannot be reconciled with a  $\Delta T/T \sim 10^{-5}$ . Obviously for much larger masses the fluctuations are much smaller.

Inflation provides a natural answer to *both* questions: the temperature anisotropies are caused by small inhomogeneities in the matter density which originated in the quantum fluctuations during the inflationary era as described in section 3.1.1 above. These density perturbations are given by eqn. (3.7) with physical wavelengths that are deep inside the Hubble radius and therefore were in causal contact during inflation (see fig.(1)). When these wavelengths cross the horizon (becoming super-horizon) during inflation, they are no longer affected by microphysical processes, but carry the initial correlations that they had while inside the Hubble radius. When they re-enter the Hubble radius right before the LSS, these density fluctuations provide anisotropies in the gravitational potential. As the photons fall in these anisotropic potential wells their wavelengths are redshifted, regions with larger densities provide larger gravitational potential and photons are redshifted more and are therefore *cooler*. These regions were in causal contact *during* inflation, became causally disconnected from any physical process until they re-entered again the Hubble radius, carrying the original correlations. Although there are many details in the relation between temperature and density anisotropies [6, 4, 3] this simple argument illustrates some of the most important physics for the anisotropies on the scales measured by COBE. A detailed analysis [6, 4, 3] yields

$$\frac{\Delta T}{T_0} \sim \frac{1}{3} \frac{\Delta \rho}{\rho} \Big|_{LSS} \quad (3.31)$$

The *main point* of this discussion and the reason for delving on this subject, is to highlight that the CMB reveals information on processes that occurred *very early*, for example during inflation, when the physical wavelengths of the perturbations that generate the temperature anisotropy first crossed the horizon, or *very late*, near recombination right after they re-entered. To precisely highlight this point we have purposely studied in section 3.1 the influence of a phase transition on the power spectrum of density perturbations, and therefore by eqn. (3.31) on the temperature fluctuations. That is to say, and we emphasize, that if the CMB reveals *any* observable consequences of phase transitions—the main theme of this lecture—these are *not* part of the standard model: either these phase transitions occurred at the time of inflation (perhaps some GUT?) or at a very low energy scale of  $\mathcal{O}(\text{eV})$ . The acoustic peaks in the multipole expansion of the temperature anisotropies can give *indirect* information on possible phase transitions through constraints on  $\Omega_b h^2$  and the cosmological parameters [1].

### 3.6 Galaxy formation and on to Stars...

The temperature anisotropies measured in the CMB give the clue to the origin of large scale structure and the formation of galaxies. As described above, the temperature fluctuations of the CMB reflect fluctuations in the density of matter. The currently accepted scenario for the formation of galaxies and large scale structure begins with the growth of small (linear) perturbations in the density under the relentless action of gravity. To understand the main ideas in a simplified manner, consider a small fluctuation  $\delta \rho$  in a background of constant density  $\rho_0$ . A region of larger density has a larger gravitational potential which in turn causes this region to become denser, i.e, gravity tends to make this overdense region even more overdense. The dynamical time scale for the free-fall collapse of this region is

$$t_{ff} \sim \frac{1}{\sqrt{G_N \rho_0}} \sim \frac{1}{H} \quad (3.32)$$

with  $G_N = 1/M_{Pl}^2$  being Newton’s gravitational constant. However a change in density induces a proportional change in pressure which tends to restore hydrostatic equilibrium. The proportionality constant is determined by the speed of sound,

$$\delta p = c_s^2 \delta \rho \quad (3.33)$$

Consider a perturbation of wavelength  $\lambda$ , if the time it takes a pressure wave to restore hydrostatic equilibrium over this wavelength is *smaller* than the free-fall time (3.32), then the restoring force from the pressure wave prevents the gravitational collapse. On the other hand if the free-fall time for collapse is *shorter* than the time scale for the pressure wave to restore equilibrium over the distance  $\lambda$ , gravitational collapse is unhindered. The balance between these two time scales determines the Jeans wavelength

$$\lambda_J \sim \frac{c_s}{\sqrt{G_N \rho_0}} ; \quad \begin{cases} \lambda > \lambda_J & \Rightarrow \text{collapse} \\ \lambda < \lambda_J & \Rightarrow \text{no collapse} \end{cases} \quad (3.34)$$

this is the *Jeans instability*. In a non-expanding geometry this instability leads to the exponential growth of density perturbations for  $\lambda > \lambda_J$ , but in an expanding geometry the instability has to catch up with the expansion and as a result small perturbations grow as a power law with time [39]. In particular for a matter dominated Universe (as is the case after recombination) the density profile for  $\lambda > \lambda_J$  grows in time as

$$\frac{\delta \rho(t)}{\rho_0} \sim a(t) \propto t^{\frac{2}{3}} \quad (3.35)$$

or equivalently

$$\frac{\delta \rho(t)}{\rho_0} \sim (1+z)^{-1} \quad (3.36)$$

To get an idea of the order of magnitude of the Jeans scale it is illuminating to compute the Jeans mass (mass contained in a volume of radius  $\lambda_J/2$ ) at the time of recombination. At this time most of the matter is in the form of hydrogen with an (adiabatic) speed of sound  $c_s^2 = 5k_B T/3m_H$  leading to [39]

$$M_J = \frac{\pi \lambda_J^3 \rho_0}{6} \sim 1.6 \times 10^5 \frac{M_\odot}{(\Omega_0 h^2)^{\frac{1}{2}}} \quad (3.37)$$

which is the size of a typical globular cluster.

Since at the LSS  $\delta \rho/\rho_0 = 3\Delta T/T \sim 10^{-4}$  at a redshift  $z_{LSS} \sim 1100$ , the argument above suggests that density perturbations become non-linear (their amplitude becomes of  $\mathcal{O}(1)$ ) at redshift of  $\mathcal{O}(1)$ , which is consistent with observations of star-forming regions [39]. Thus the temperature fluctuations in the CMB give direct confirmation of the paradigm of structure formation based on the gravitational instability of primordial density perturbations.

The main points of the analysis provided in this section are: i) to argue that the primordial density fluctuations that determine the temperature fluctuations of the CMB through (3.31) provide the seeds for structure formation. Any information from a primordial phase transition that is imprinted in the anisotropies of the CMB is also imprinted in the initial power spectrum of density perturbations that seed large scale structure formation. ii) to highlight that when the pressure vanishes, gravitational collapse on large scales goes unhindered. This last observation relates to the previous discussion of the formation of primordial black holes during the QCD phase transition, which if first order implies an anomalously small (if not vanishing) speed of sound.

### 3.7 Stellar Evolution 101: QGP at the core of Pulsars?

The basic Jeans gravitational instability is also at the heart of star formation. *Protostars* condense from giant molecular (hydrogen) gas clouds [40]. A solar mass protostar condenses in typical star forming regions

with temperatures  $T \sim 20 K$  and densities  $\gtrsim 10^{-16} g/cm^3$  the gravitational contraction of the cloud heats up the gas until the temperature reaches  $\sim 10^7 K$  when thermonuclear fusion of hydrogen into helium generates enough energy and pressure to halt the collapse. The threshold mass for a star to undergo thermonuclear fusion is about  $0.08 M_\odot$ . Stars with smaller masses do not attain the temperature to ignite hydrogen and the gravitational pull is counterbalanced by electron degeneracy, these “failed” stars are called *brown dwarfs*. Solar mass type stars live on the main sequence for about 10 billion years and spend most of their lives burning hydrogen into helium mainly through the three branches of the pp (proton-proton) chain and more massive stars also produce helium through the C(arbon)N(itrogen)O(xygen) chains [40]. When hydrogen is depleted, gravitational contraction begins again until the temperature reaches about  $10^8 K$  when the thermonuclear fusion of helium begins at the core while a shell of hydrogen still burns outside the core. This helium burning stage produces carbon (through the miracle of the triple alpha process) and oxygen. Computer simulations [40] show that stars with masses up to  $\sim 8M_\odot$  burn hydrogen and helium but the temperatures attained at the core are not high enough to ignite carbon. These stars (the sun is one of them) end up their life cycles as *white dwarfs*, with a degenerate CO core, the gravitational pull is counterbalanced by the Fermi degeneracy pressure of electrons. Typical radii and densities of these stars are  $R \sim 10^4 \text{ Km}$ ;  $\rho \sim 10^6 gr/cm^3$ . The maximum mass for a stellar object to be in hydrostatic equilibrium balanced by Fermi degeneracy pressure is given by the Chandrasekhar limit  $\sim 1.4 M_\odot$ . When the density is such that the Chandrasekhar limit is reached, electrons at the top of their Fermi surface become ultrarelativistic and the equation of state is softer. Stars with masses  $> 8 - 10 M_\odot$  evolve through all the stages of nuclear burning beginning with hydrogen, continuing with helium, carbon, neon, oxygen and silicon burning (photodisintegration at  $T \sim 3.5 \times 10^9 K$ ) which ends in the iron group elements with an  $^{56}Fe$  core and concentric shells (“onion structure”) of silicon, neon, oxygen, carbon, helium and hydrogen. Since Fe has the largest binding energy per baryon, thermonuclear fusion cannot proceed further. For stars with masses  $> 10M_\odot$  the iron core reaches the Chandrasekhar limit for support by electron degeneracy and is on the limit of gravitational collapse. There are two main factors that trigger the collapse [40, 41, 42]: i) the temperature of the core is now  $\sim 8 \times 10^9 K$  enough to photodisintegrate iron group elements by the reaction



ii) the Fermi energy of the degenerate electrons becomes larger than the neutron-proton mass difference  $\sim 1.3\text{Mev}$  and is therefore large enough for electron capture by protons



this is the process of neutronization. As the electrons that support the gravitational pull with their Fermi pressure are captured, hydrostatic equilibrium falters and the core begins to collapse on a dynamical (free fall) time scale given by eqn. (3.32). With the density of the core  $\sim 10^9 g/cm^3$  the free fall time scale for collapse is  $\sim 1\text{msec}$ . As the collapsed core reaches nuclear matter density, it becomes highly incompressible and its equation of state stiffens. The infalling matter from the outside shells bounces from the incompressible core and a shock wave is formed. This shock blows off the outer layers resulting in a Supernova (core-collapse or Type II) explosion. The details of the explosion and the shock are very complex and involve neutrino transport, convection etc. For more details the reader is referred to [40, 41, 42].

What happens after this depends on the mass of the progenitors. Current understanding based on numerical evolution [40, 41, 42] suggests that for stars with masses up to about  $30M_\odot$  the final result is a neutron star, while for masses larger than this the collapse probably leads to the formation of a black hole. When the supernova explosion leads to a neutron star, an important feature with observational consequences is that during the process of neutronization of the iron core with the Chandrasekhar mass  $\sim 1.4M_\odot$  most of the  $10^{57}$  protons present in the core are converted to neutrons and  $\sim 10^{57}$  neutrinos each of about  $10\text{Mev}$  are released and carry most (up to 99%) of the energy  $\sim 10^{53}\text{ergs}$ . When the density of the collapsing core reaches about  $4 \times 10^{11} g/cm^3$ , neutrons begin to *drip* out of the nuclei, this is the *neutron drip line* and the

collapsing core becomes a gigantic neutron. Typical neutron stars have masses in the range  $1.4 - 2M_{\odot}$  with typical radii  $\sim 10 \text{ km}$ . The most direct evidence for neutron stars are *pulsars* which are believed to be highly magnetized ( $B \sim 10^{12} \text{ G}$ ) rotating neutron stars [43, 44]. Pulsar periods range from about a millisecond up to a second.

The equation of state for neutron stars for densities *below* nuclear matter  $\rho_n \sim 2 \times 10^{14} \text{ g/cm}^3$  is fairly well understood [45, 46], while for densities above  $\rho_n$  there is the possibility of hyperon rich matter, pion and or kaon condensates, muons, and other exotica [43, 44, 45, 46]. Modern theories of superdense nuclear matter [45, 46, 43, 44], predict a composition for neutron stars that is depicted qualitatively in fig.(2) below.

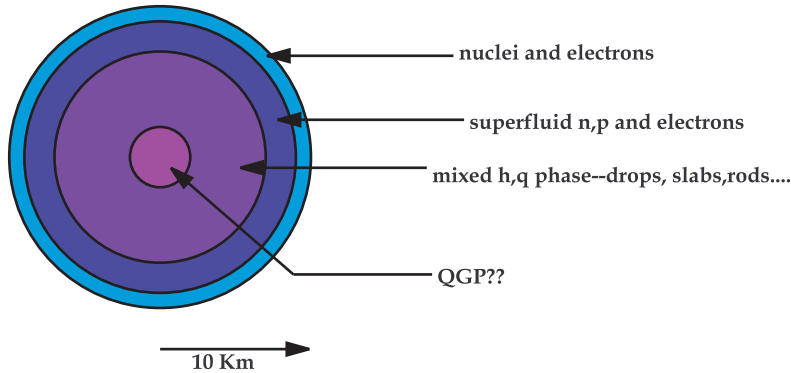


Figure 2: Neutron star composition.

A crust of ( $^{56}\text{Fe}$ ) nuclei, electrons and neutrons, followed by an internal region of neutron and proton superfluids with the possibility of pion and kaon condensates and hyperons. But more importantly for this discussion, current ideas suggest the possibility of a mixed phase of hadrons and quarks, characterized by geometric structures (a consequence of the competition between nuclear and Coulomb forces) and ultimately a core of *deconfined* quarks and gluons with  $T \leq 1 \text{ Mev}$  and  $\rho \sim 3 - 5\rho_n$ , i.e, the core is conjectured to be a *cold, dense Quark Gluon Plasma*.

Recently the interesting possibility of novel color superconducting phases of cold and dense QCD has been proposed and we refer the reader to several review articles on the subject for details on these fascinating aspects [47].

In a very tantalizing recent article Glendenning and Weber [48] proposed that a phase transition to quark matter can provide a potential explanation for the anomalous distribution of pulsar frequencies in low mass X-ray binaries (LMXBs). Observations of the pulsar frequencies in LMXBs by the Rossi X-ray Timing Explorer reveal a spike at a frequency  $\sim 300 \text{ Hz}$ . We will describe this fascinating possibility below along with the current experimental efforts to map the QCD phase diagram with ultrarelativistic heavy ion collisions.

The physics is different for Type Ia Supernovae that are currently at the center of the discussion of their use as standard candles to study the cosmological constant [49]. These are conjectured to be CO white dwarfs in a binary system. The white dwarf accretes mass from its companion until its own mass becomes just below (a few percent) of the Chandrasekhar limit. Current understanding suggests that at this point the CO core begins thermonuclear burning under degeneracy conditions. This results in runaway burning since in the Fermi degenerate situation the pressure is almost independent of the temperature (just as in the helium flash). The temperature increase at almost constant pressure leads to a runaway thermonuclear burning that results in the explosion of the star [42]. What makes these supernovae so special is that their composition and mass at the time of the explosion is the same for all Type Ia Supernovae and this feature may explain their similar light curves [50].

### 3.8 Executive Summary: observational consequences of cosmological phase transitions?

The focus of the review of big bang cosmology as well as the astrophysics of (compact) stars is to highlight where and when there could be observational consequences of the phase transitions predicted by the standard model of particle physics. The picture that emerges from this brief tour through the early Universe, is that while current CMB measurements and large scale surveys have the potential for revealing evidence for *inflationary* phase transitions the observable evidence for a standard model phase transition is at best *indirect*. I have argued that inflationary phase transitions, perhaps taking place at the GUT scale could leave an imprint in the power spectrum of temperature anisotropies, for example a red tilt as a consequence of spinodal instabilities [9]. Or as argued in ref. [14] a step-like feature in the power spectrum of temperature anisotropies or in the power spectrum of galaxy clusters may be produced by an inflationary phase transition in a supersymmetric theory. Either proposal however, lies beyond the *standard model* and at energy scales unlikely to be probed by any current or future accelerator. The main “problem” with detecting phase transitions with the CMB or large scale surveys is that the fluctuations that can seed temperature and density inhomogeneities were generated very *early*, during inflation, i.e, at an energy scale  $\sim 10^{16}$  Gev, or very *late* during recombination, i.e, at an energy scale  $\sim 0.3$  eV. As is clear from fig.(1) scales of cosmological relevance today, say from  $\sim 10$ Mpc up to the Hubble radius  $\sim 3000$ Mpc, were super-horizon, hence decoupled from the microphysics at the time of the EW or QCD phase transitions.

The *indirect* evidence for standard model phase transitions is contained in the baryon to photon ratio, i.e, the baryon asymmetry and in the possibility of primordial black holes or inhomogeneous nucleosynthesis caused by the QCD phase transition. As argued above, it now seems clear that the standard Electroweak theory cannot describe consistently baryogenesis because of the smallness of the CP violating parameter(s) as well as the large Higgs mass. This analysis leaves the responsibility for observational consequences of standard model phase transitions squarely on the shoulders of QCD!. A strong first order phase transition from a QGP to a hadron phase can lead to the formation of primordial black holes because the speed of sound becomes anomalously small thus gravitational collapse of solar mass clumps is unhindered. There is the possibility of inhomogeneities in the baryon density leading to inhomogeneous nucleosynthesis with the tantalizing possibility of explaining the new bounds on  $\Omega_b h^2$  from Boomerang and Maxima. There is also the possibility for the formation of strangelets or strange quark nuggets that could be a component of the cold dark matter. As described above most of these possibilities rely on the details of the QCD PT and the parameters of QCD that determine the main dynamical aspects of the transition. While the lattice gauge theories program has the potential for computing many of these quantities, it is clearly important to study *experimentally* the phase transitions of the standard model. As mentioned above the *direct study* of the EWPT is certainly out of the reach of current and most certainly near future accelerators: to achieve the PT temperature  $T \sim 100$  Gev requires an energy density  $\varepsilon \sim 10^{11} \rho_n$ . The QCD phase transition is perhaps the *only* phase transition of the standard model that *can and is being* studied with accelerators. At the QCD PT temperature  $T \sim 200$  Mev the energy density required is  $\varepsilon \sim 2 - 4 \rho_n$  which is the energy density achieved in *ultrarelativistic heavy ion collisions*. I now describe the current (and future) program to study the QCD phase transition(s) with ultrarelativistic heavy ion collisions, as well the recent fascinating suggestion that there could be observable hints of quark matter in the core of pulsars.

## 4 Relativistic heavy ion collisions and pulsars open a window to the early Universe:

The program of relativistic heavy ion collisions whose primary goal is to study the phase diagram of QCD began almost two decades ago with the fixed target heavy ion programs at the AGS at Brookhaven and the SPS at CERN. Recently [34, 35] a summary of the results of these efforts mainly through the  $Pb + Pb$  experiments at SPS-CERN provided very exciting “evidence” in favor of the existence of the QGP. As impressive as this body of evidence is, the consensus in the field is that while the evidence is very suggestive

it is far from conclusive. As SPS shuts down to pave the way for the forthcoming Large Hadron Collider wherein the Alice program will continue the search for the QGP, the torch now passes to the R(elativistic) H(eavy)I(on)C(ollider) at BNL.

## 4.1 RHIC and LHC seek the QGP: the big picture

The Relativistic Heavy Ion Collider (RHIC) at BNL is currently studying  $Au + Au$  collisions with center of mass energy  $\sqrt{s} \sim 200 \text{AGev}$  and luminosity  $\sim 10^{26} \text{cm}^{-2} \text{s}^{-1}$ . The future ALICE heavy ion program at LHC is expected to study  $Pb+Pb$  collisions with c.m. energies up to  $\sqrt{s} \sim 5 \text{ATev}$  and luminosities  $\sim 10^{27} \text{cm}^{-2} \text{s}^{-1}$ . In these collisions the heavy nuclei can be pictured in the CoM frame as two Lorentz contracted pancakes, for example for  $Au + Au$  collisions the size of each “pancake” in the direction transverse to the beam axis is about 7 fm. At RHIC and LHC energies most of the baryons are expected to be carried away by the receding pancakes (the fragmentation region) while in the region of the collision a large energy (density) is deposited in the form of quark pairs and gluons. At least two important mechanisms for energy deposition in the collision region are at work [51, 52, 53]: i) the establishment of a strong color electric field (flux tube) that eventually breaks up into quark-antiquark pairs when the energy in the field is larger than the pair production threshold and ii) the partons (quarks and gluons) inside the colliding nuclei interact and redistribute their energy in a “parton cascade” [54]. An estimate of the energy deposited in the collision region has been provided by Bjorken [55]

$$\epsilon = \frac{1}{\tau_0 \pi R_A^2} \frac{dE_T}{dy} \quad (4.1)$$

with  $\tau_0 \sim 1 \text{fm}/c$ ,  $R_A \sim 7 \text{fm}$  for Au and  $dE_T/dy$  is the transverse energy per unit rapidity which is *measured*. At RHIC the transverse energy per unit rapidity is expected to be in the range 500 – 900Gev, giving for the energy density  $\epsilon \sim 4 - 6 \text{Gev}/\text{fm}^3$  translating this value into the temperature of a quark-gluon gas leads to  $T \gtrsim 400 \text{Mev}$  larger than the expected critical temperature  $T_c \sim 160 \text{Mev}$ . The evolution of the parton distribution functions reveals that thermalization of quarks and gluons occurs on time scales  $\mathcal{O}(0.3 - 0.7) \text{fm}/c$  with gluons thermalizing first [51, 52]. After the quark-gluon plasma achieved LTE, the evolution is conjectured to be described by hydrodynamic expansion [56]. As the QGP expands and cools, the temperature falls near the critical temperature and the confinement and chiral phase transitions occur. Upon further cooling the quark-gluon plasma hadronizes, the hadrons rescatter until the hadron gas is dilute enough that the mean free path is larger than the mean distance between hadrons. At this point hadrons “freeze-out” and stream out freely to the detectors from this *last scattering or freeze-out surface*. This picture is summarized in fig. (3) below.

Current estimates based on this picture and on detailed numerical evolution [57] suggest that at RHIC the quark gluon plasma lifetime is of order  $\sim 10 \text{fm}/c$  while the total evolution until freeze-out is  $\sim 50 - 100 \text{fm}/c$ .

### 4.1.1 Hydro, LGT and the EoS:

Although the evolution of the quark gluon plasma from the initial state described by the parton distribution of the colliding nuclei until freeze-out of hadrons clearly requires a non-equilibrium description, a hydrodynamic picture of the evolution is both useful and experimentally relevant [56]. In the approximation in which quarks and gluons are strongly coupled in the sense that their mean free paths are much smaller than the typical wavelength for the variation of collective phenomena, the QGP can be described as a *fluid* in LTE. Hydrodynamics results from the conservation laws applied to the fluid form of the energy momentum tensor and the conserved currents. In particular for a fluid in LTE, the energy momentum tensor is of the form

$$T^{\mu\nu} = (\epsilon + p)u^\mu u^\nu - pg^{\mu\nu} \quad (4.2)$$

with  $\epsilon, p$  the energy density and pressure respectively,  $g^{\mu\nu}$  is the metric and

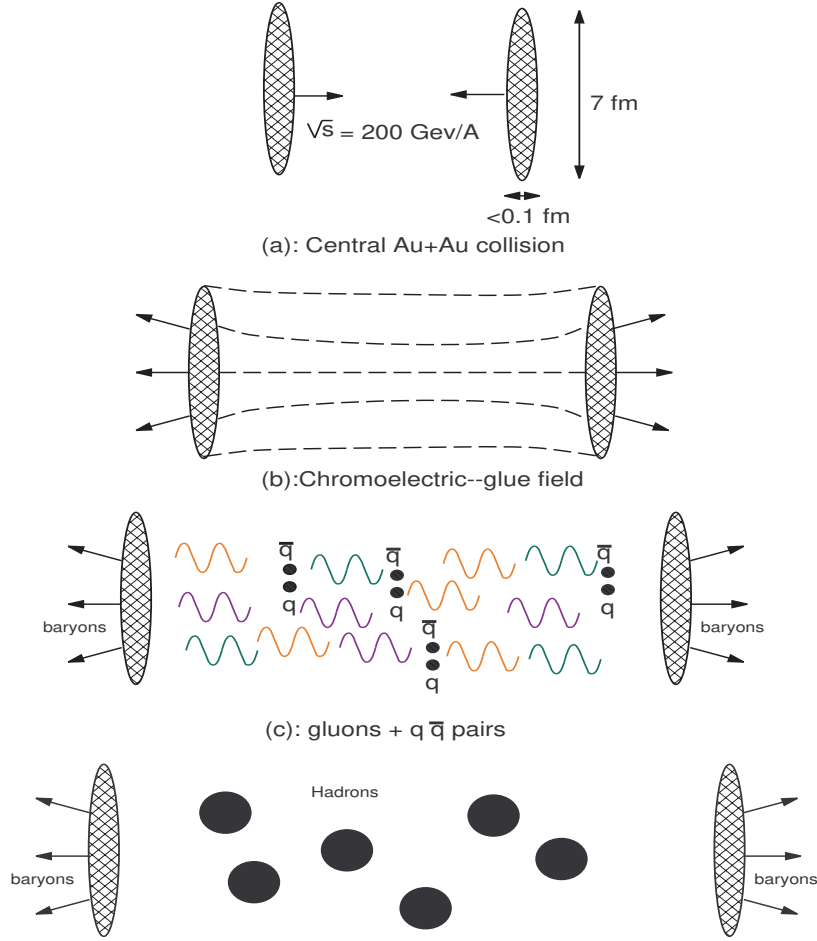


Figure 3: Heavy Ion Collisions.

$$w^\mu = \gamma(x)(1, \vec{v}(x)) \quad (4.3)$$

is a local 4-velocity vector with  $\gamma(x)$  the local Lorentz contraction factor. In this description the dynamical evolution of the fluid is obtained from the conservation laws of energy-momentum, baryon number and entropy [53, 56] and to close the set of equations one needs an equation of state  $p = p(\varepsilon)$ .

In order to make a definite connection with the cosmological setting as well as for its simplicity and usefulness to describe qualitatively the expansion and cooling of the QGP we now briefly summarize Bjorken's model for longitudinal expansion [53, 55, 56]. There are three important ingredients in Bjorken's models: i) the "central rapidity" region where the energy deposited and the formation of the QGP takes place is well separated from the "fragmentation region" which is the region of the receding pancakes where most of the baryons are (see fig.(3)). ii) The thermodynamic variables are invariant under boosts along the beam (longitudinal) axis, this is based on the observation that the particle distributions are invariant under these boosts in the "central rapidity region" and iii) the expansion only occurs along the beam axis, i.e, longitudinal expansion. In the baryon free region, local thermodynamics implies that the entropy density in the local



rest frame of the fluid is related to the energy density and pressure as

$$\varepsilon + p = Ts \quad (4.4)$$

It is convenient to introduce the space time rapidity variable  $\eta$  and proper-time  $\tau$

$$\eta = \frac{1}{2} \ln \left[ \frac{t+z}{t-z} \right] \quad ; \quad \tau = \sqrt{t^2 - z^2} \quad (4.5)$$

with  $z$  the coordinate along the beam axis (longitudinal). Introducing the fluid rapidity  $\theta$  by writing the local velocity (4.3) as

$$u^\mu = (\cosh(\theta), 0, 0, \sinh(\theta)) \quad (4.6)$$

Furthermore Bjorken's model assumes the fluid to be composed of free streaming particles for which  $v_z = z/t$  in which case the fluid rapidity  $\theta$  becomes the space-time rapidity  $\eta$ . Boost invariance along the longitudinal direction entails that  $\varepsilon, p, s, T$  are all functions of proper time only (here  $s, T$  are the entropy density and temperature [55, 56]).

The energy-momentum conservation equation  $\partial_\mu T^{\mu\nu}$  leads to two equations by projecting along the direction  $u^\mu$  and perpendicular to it using the projector  $g^{\mu\nu} - u^\mu u^\nu$ . Under the assumption that the central region is baryon free, the conservation of entropy and energy and momentum lead to the following equations (for details see [56, 21, 53, 55])

$$\frac{d\varepsilon(\tau)}{d\tau} + \frac{1}{\tau}(\varepsilon + p) = 0 \quad (4.7)$$

$$\frac{ds(\tau)}{d\tau} + \frac{s}{\tau} = 0 \quad (4.8)$$

Assuming an equation of state  $p(\tau) = p(\varepsilon(\tau))$  and combining eqns. (4.7,4.8) with the thermodynamic relation (4.4) (for baryon free plasmas) one finds that the evolution of the temperature is given by

$$\frac{\tau}{T} \frac{dT}{d\tau} = -c_s^2 \quad ; \quad c_s^2 = \frac{dP}{d\varepsilon} \Big|_s \quad (4.9)$$

Which for constant speed of sound results in the cooling law

$$T(\tau) = T_0 \left( \frac{\tau_0}{\tau} \right)^{c_s^2} \quad (4.10)$$

Obviously the form of the equation (4.7) is similar to the energy conservation equation in a homogeneous and isotropic metric given by (2.8) with the expansion rate  $\dot{a}/a = 1/3\tau$  when the proper time  $\tau$  is identified with the comoving time  $t$  in the cosmological setting. The similarity becomes even more remarkable for the case of the QGP being modelled as a radiation fluid (which is expected to be a good approximation at high temperature) since in this case  $c_s^2 = 1/3$  and the connection with a radiation dominated cosmology with scale factor  $a(t) \propto t^{1/3}$  is evident.

To find the general evolution equations for the QGP under the conditions specified above, an equation of state is needed.

It is at this stage where the connection with the lattice gauge theory (LGT) program is made. LGT obtains the thermodynamic functions *in equilibrium* and these are input in the hydrodynamic description as local functions of space-time under the assumption of LTE. Fig. (4) below is an example of recent results

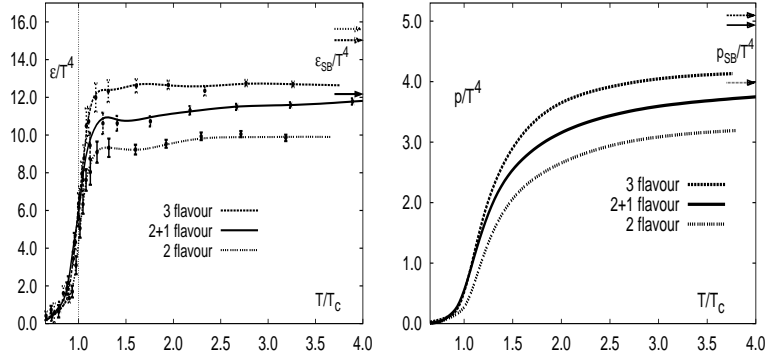


Figure 4:  $\varepsilon/T^4$  and  $p/T^4$ , vs  $T/T_c$  for a  $16^3 \times 4$  lattice. From [58].

from LGT for the energy density and pressure (both divided by  $T^4$  to compare to a free gas of massless quarks and or gluons) as a function of  $T/T_c$  with  $T_c = 170$  Mev.

It is clear from these figures that there is a sharp decrease in the energy density and pressure at  $T = T_c$ , the value of the energy density at  $T_c$  is, from the figure  $\varepsilon_c \sim 6T_c^4$ . Furthermore the large temperature behavior is *not quite* given by the Stephan-Boltzmann law ((SB) in the figures), suggesting that even at large temperatures the plasma is not described by free quarks and gluons up to temperatures  $T \sim 4.0T_c \sim 700$  Mev. This discrepancy is currently explained in terms of quasiparticles rather than free particles (see below). Nevertheless, what transpires clearly from these figures is that for temperatures  $T > T_c$  the plasma is approximately a gas of almost free massless quarks and gluons, while for  $T \ll T_c$  the plasma is dominated by heavy particles. This is the picture that deconfinement-confinement phase transition suggests.

A hydrodynamic description combined with the non-perturbative lattice gauge theory program to extract the EoS of the QGP provide a basic quantitatively reliable picture of the dynamical evolution of the QGP. The approximation of ideal (or perfect) hydrodynamics can be relaxed by considering *viscous* hydrodynamics by including the bulk and shear viscosity in the energy momentum tensor [56, 59].

## 4.2 Thermalization, quasiparticles and the EoS:

The initial stages of evolution of the QGP beginning from the distribution of partons (quarks and gluons) in the colliding nuclei is studied with a semiclassical transport approach that includes perturbative QCD cross sections with screening corrections [54]. These studies reveal that gluons and quarks thermalize on time scales  $< 1fm/c$  with gluons thermalizing first. While a classical (or semiclassical) transport approach may not be completely justified in this regime, a qualitative and quantitative idea of the relaxation time scales can be obtained by *assuming* a thermalized state and studying how a small departure from equilibrium relaxes. The relaxation rate is given by  $\Gamma = n\sigma$  with  $n$  the particle density and  $\sigma$  a typical scattering cross section. Consider the relaxation of quarks in a bath of gluons at temperature  $T$ , one gluon exchange yields a typical cross section

$$\sigma \sim \frac{\alpha_s^2}{T^2} \quad (4.11)$$

with  $\alpha_s = g^2/4\pi$  and  $g$  is the gauge coupling constant and we have assumed that the typical energy of the exchanged gluon is  $\sim T$ . For  $T \gg m$  with  $m$  the typical masses,  $n \propto T^3$  leading to

$$\Gamma \sim \alpha_s^2 T \quad (4.12)$$

Gluons of typical energy  $T$  are hard and lead to smaller cross sections, while the exchange of soft gluons leads to larger cross sections and is more efficient for thermalization. However soft gluons are screened by the medium. The estimate above, eqn. (4.11) is reliable for hard gluon exchange, but overlooks the fact that *soft* longitudinal gluons are Debye screened. A careful calculation [60] reveals that the Debye screening length  $m_D \sim gT$  therefore the denominator in eqn. (4.11) must be replaced by  $T^2 \rightarrow g^2 T^2$ . Furthermore, while longitudinal (electric) gluons are Debye screened, transverse (magnetic) gluons are only *dynamically screened* by Landau damping [61, 60]. Including these screening effects it is found that the quark relaxation rate is given by [62]

$$\Gamma \sim \alpha_s T \ln \left( \frac{1}{g} \right) \quad (4.13)$$

for  $\alpha_s \sim 0.3$ ;  $T \sim 300\text{Mev}$  one finds the typical relaxation time  $\tau_{rel} = \Gamma^{-1} \sim 0.8 - 1\text{fm}/c$ .

The main point in bringing up this estimate is to highlight the fact that in a medium there are many-body effects that screen or “dress” the particles, and as a result, even for high temperatures the plasma is *not* described by a free gas of quarks and gluons, but in terms of “dressed” weakly interacting *quasiparticles*. In a thermalized QGP these quasiparticles have a typical “thermal mass” of order  $gT$  [60]. A framework to include these screening corrections consistently in the perturbative expansion has been put forth in ref. [61] and is referred to as the hard thermal loop (HTL) program. In fact the energy density and pressure obtained by the LGT program depicted in fig. (4) have been recently reproduced analytically in terms of *thermal quasiparticles* with a typical mass of order  $gT$  [63]. Thus the combination of numerical results from LGT and the analytic resummation provided by the HTL program lead to a picture of the QGP at high temperatures in terms of weakly interacting quasiparticles with thermal masses  $\sim gT$ .

### 4.3 Predictions and observations:

Several experimental signatures had been associated with the formation of the QGP [51, 64], and the heavy ion programs had focused on several of them. Here I summarize the observables that have been proposed as telltales of a QGP and the data gathered by the SPS from  $Pb + Pb$  and  $Pb + Au$  collisions, which taken together provide a hint of evidence [34, 35, 52] for the effects associated with a QGP (although many if not all of them could have alternative explanations).

#### 4.3.1 $J/\Psi$ suppression:

The  $J/\Psi$  is a  $\bar{c}c$  bound state that is very narrow and that if produced in the early stages of the collision can probe the QGP because its lifetime is longer than that of the QGP and decays into dilepton pairs which leave the plasma without scattering. The original suggestion [65] is that when the screening length of the color force is smaller than the size of the  $\bar{c}c$  bound state, this narrow resonance will “melt”. This original argument thus suggests that a suppression of the  $J/\Psi$  yield could provide information on the existence of the QGP. Alternatively a suppression could result from scattering with hard gluons in the plasma and the “dissociation” of the bound state [65]. A normal suppression of charmonium is expected on the grounds that once formed the  $\bar{c}c$  bound state interact with other nucleons inside the nucleus. This expected suppression is studied in proton nucleon collisions and extrapolated to nucleon-nucleon collisions. This is considered the “normal” suppression in contrast to the “abnormal” suppression expected from the presence of a plasma. Fig. (5) below shows the data gathered by the NA50 collaboration at the SPS-CERN [66].

This striking figure clearly reveals an “abnormal” suppression when the energy density is  $\varepsilon > 2.5\text{Gev}/\text{fm}^3$ . The energy density in this figure has been computed with Bjorken’s formula (4.1). Further analysis [34, 35] reveals that this anomalous suppression cannot be accounted for by collisional dissociation through final state hadronic interactions.

A recent report from the NA50 collaboration at CERN-SPS [67] presents the combined data for  $J/\Psi$  suppression from the NA38 and NA50 experiments. The analysis of the data reveals that while for the most

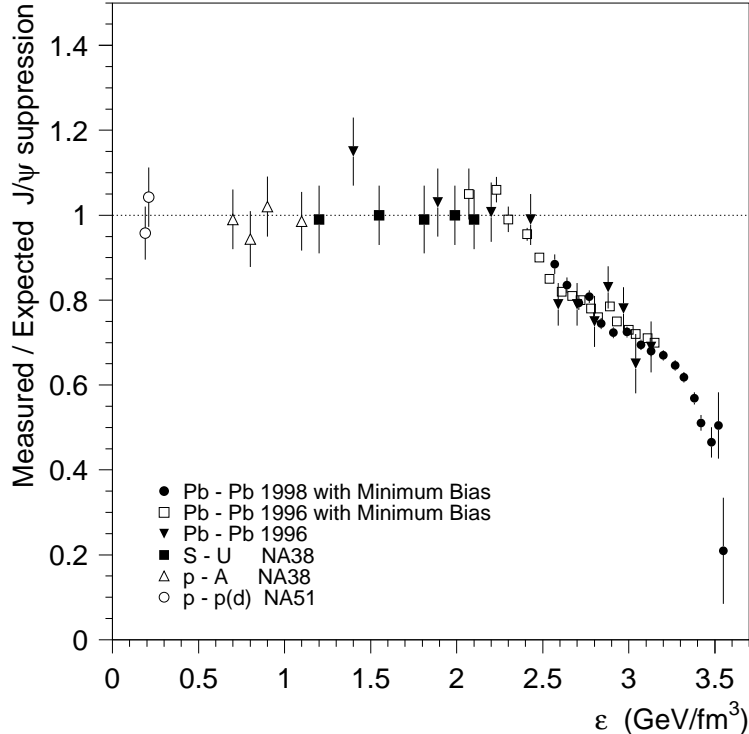


Figure 5: Anomalous  $J/\psi$  suppression as a function of the initial energy density. From [66]

peripheral (largest impact parameter) collisions the suppression can be accounted for by nuclear absorption, there is no saturation in the suppression in the most central  $Pb + Pb$  collisions and that the observed suppression pattern can be naturally understood in a deconfinement scenario. This report concludes that *the  $J/\Psi$  suppression pattern observed in the NA50 data provides significant evidence for deconfinement of quarks and gluons in  $Pb + Pb$  collisions.*

#### 4.3.2 Electromagnetic probes: dileptons and direct photons

Electromagnetic probes:  $e^+e^-$  or  $\mu^+\mu^-$  dilepton pairs and direct (prompt) photons are prime probes of the hot plasma [68], since once produced they leave the plasma without further interactions because their mean free path is *much* larger than the typical size of the plasma.

##### Dileptons:

The  $\rho$  vector meson has particular relevance in this regard because it decays into dileptons and its lifetime is  $\sim 1fm/c$ , therefore once it is produced in the hadron gas it decays *within* the hot hadronic plasma and the produced dileptons carry directly this information. Thus while dileptons produced from the decay of the  $\rho$  meson do not yield evidence of the earlier stages in the QGP, they do nevertheless offer information on the hadronic stage. Figure (6) below presents the data gathered by the CERES-NA45 collaboration for the invariant mass spectrum for electron-positron pairs from 158 AGeV  $Pb + Au$  collisions at the SPS-CERN.

The solid line represents the expected spectrum from the decays of hadrons produced in proton-nucleon and proton-proton collisions extrapolated to  $Pb + Au$  collisions and is the sum of the contributions shown in the graph. There are two remarkable features in this graph: a clear enhancement of dileptons in the region  $250 \text{ Mev} \lesssim M_{e^+e^-} \lesssim 700 \text{ Mev}$  and that instead of the  $\rho$  meson peak at  $m_\rho = 770 \text{ Mev}$  there is a broad

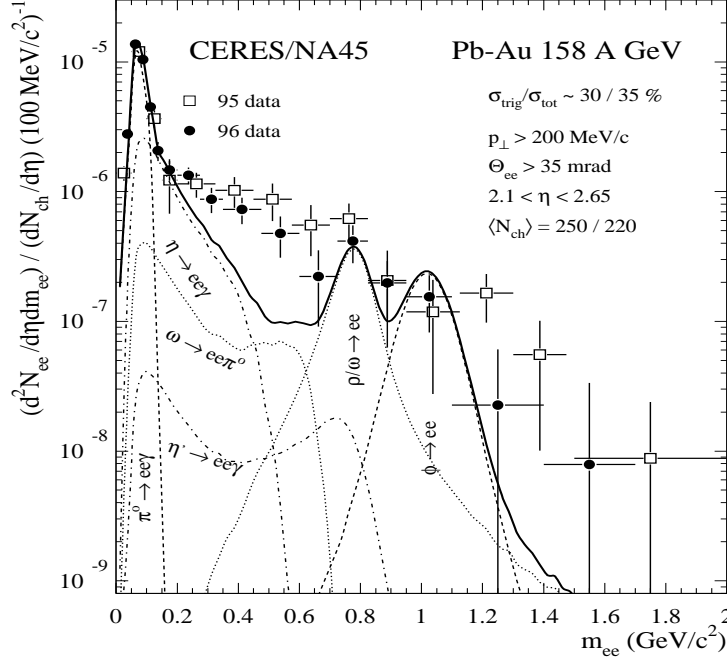


Figure 6: Invariant mass spectrum of  $e^+e^-$  pairs from  $Pb + Au$  collisions at 158 AGeV at the SPS-CERN (CERES/NA45). From [69].

distribution. The excess of dileptons in the small invariant mass region cannot be explained by charged pion annihilation [34, 35]. What is remarkable in this data is that the dilepton enhancement is *below* the putative  $\rho$  peak and that there is no hint of the  $\rho$  at 770 MeV!. The current understanding of these features is that the medium effects result in a shift in the  $\rho$  meson mass as well as a change in its width[70, 34, 35, 52]. Thus while this interpretation does not directly yield information on the QGP, it does support the picture of a hot gas of hadrons, mainly pions which is the main interaction channel of the  $\rho$  vector meson.

#### Direct photons:

Direct photons are conceptually a clean direct probe of the early stages of the QGP. Photons are produced in the QGP by several processes: gluon-to-photon Compton scattering off (anti)quark  $q(\bar{q})g \rightarrow q(\bar{q})\gamma$  and quark-antiquark annihilation to photon and gluon  $q\bar{q} \rightarrow g\gamma$  and to the *same order* (see Kapusta et. al. and Aurenche et. al. in [68]) (anti)quark bremsstrahlung  $qq(g) \rightarrow qq(g)\gamma$  and quark-antiquark annihilation with scattering  $q\bar{q}q(g) \rightarrow q(g)\gamma$ . Detailed calculations including screening corrections [68] reveal that direct photons from the QGP could provide a signal that could be discriminated against that from the hadronic background. This work indicates the theoretical feasibility of direct photons as direct probes of the early stages of the QGP.

Recently the WA98 collaboration at SPS-CERN reported their analysis for the *first* observation of direct photons from  $Pb + Pb$  collisions with  $\sqrt{s} = 158 AGeV$  [72]. Their data is summarized in the fig.(7) below.

The transverse momentum distribution of direct photons is determined on a statistical basis and compared to the background photon yield predicted from a calculation of the radiative decays of hadrons. The most interesting result is that a significant excess of direct photons beyond that expected from proton-induced reaction at the same  $\sqrt{s}$  is observed in the range of transverse momentum greater than about 1.5 GeV/c in

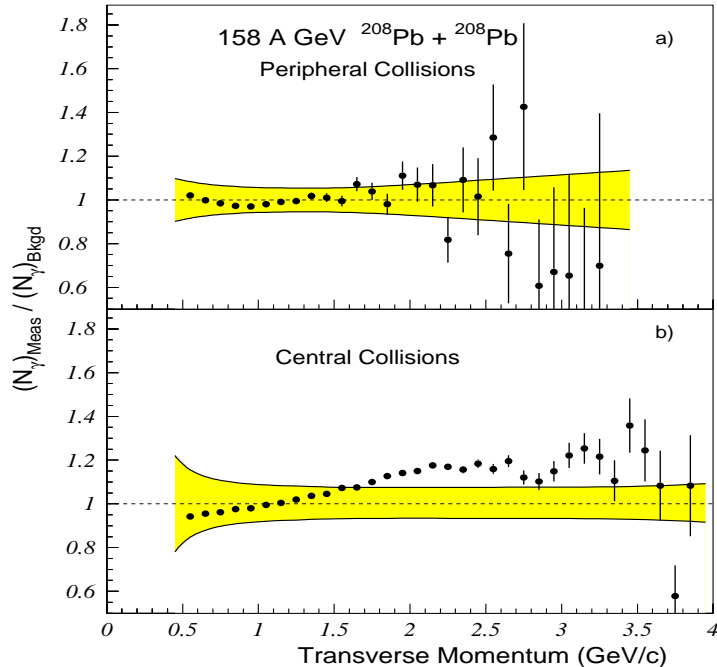


Figure 7: Ratio of total measured yield of direct photons to hadronic background vs. transverse momentum from  $Pb + Pb$  at 158 AGeV for peripheral and central collisions. From [72].

central collisions.

A detailed analysis of the data and the theoretical expectations based on the calculations of direct photons from an equilibrated QGP was recently performed [71]. The conclusions of that analysis is that while it is not clear if SPS has reached the energy density to form the QGP, the data supports indications of a hot and dense phase that could be the precursor of the QGP.

More recently [73] it has been suggested that non-equilibrium effects in an expanding QGP formed in RHIC collisions could lead to an enhancement of direct photons in the region of transverse momentum  $p_T \gtrsim 2$  Gev.

### 4.3.3 Strangeness enhancement

Strangeness enhancement along with chemical equilibration are some of the earliest proposals for clear signatures of the formation of a QGP [74]. The main idea is based on the estimate that the strangeness equilibration time in a hot QGP is of the same order as the expected lifetime of the QGP ( $\sim 10 fm/c$ ) produced in nucleus-nucleus collisions. Two important aspects of this estimate make strangeness enhancement a prime candidate: if strangeness attains chemical equilibrium in the QGP, this equilibrium value is significantly higher than the strangeness production in nucleon-nucleon collisions. Also strangeness production through hadronic rescattering or final state interactions was estimated to be negligibly small [74]. In the QGP, color deconfinement leads to a large gluon density that leads to the creation of  $s\bar{s}$  pairs, furthermore chiral symmetry makes the strange quark lighter thus lowering the production threshold. This situation is in contrast to the case of hadronic rescattering or final state interactions where the production of pairs of strange quarks has large thresholds and small cross sections [34, 35]. The usual measure of strangeness

enhancement is through the ratio

$$\lambda_s = \frac{2\langle\bar{s}s\rangle}{\langle\bar{u}u + \bar{d}d\rangle} \quad (4.14)$$

Fig. (8) below displays  $\lambda_s$  as a function of  $\sqrt{s}$  the energy of the collision for nucleon-nucleon as well as nucleus-nucleus collisions ( $S + S, S + Ag, Pb + Pb$ ) at SPS.

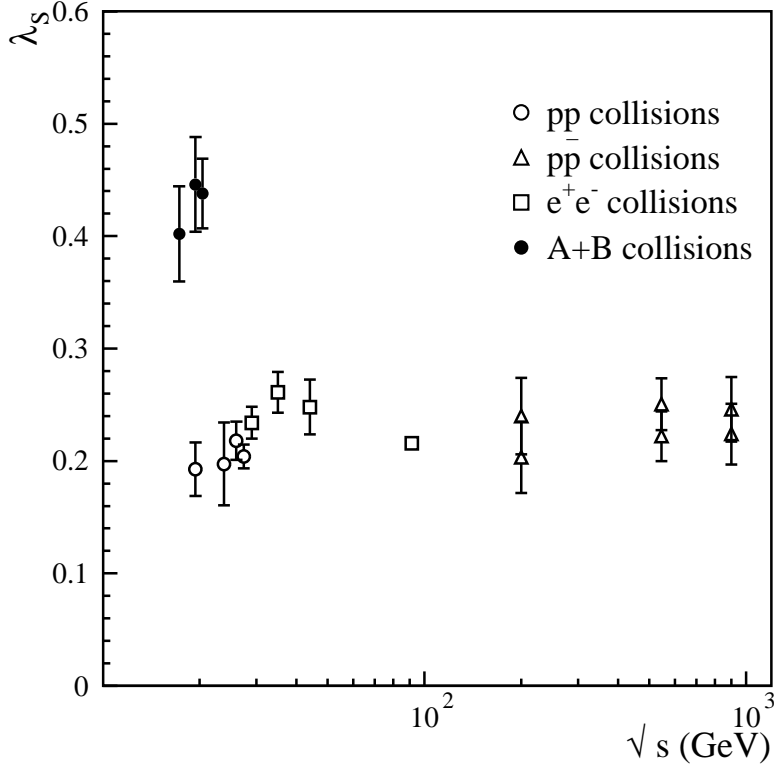


Figure 8: The ratio  $\lambda_s$  as a function of  $\sqrt{s}$ , the energy of the collision for nucleon-nucleon and nucleus-nucleus collisions. From [75]

It is clear that nucleus-nucleus collision is creating a different environment that enhances the formation of strangeness. As mentioned above, and confirmed by detailed numerical evolution of kinetic models [76], the enhancement *cannot* be explained by hadronic scattering. Thus the enhancement displayed by fig. (8) provides a very exciting hint that nucleus-nucleus collisions at SPS are creating a hot state of matter.

#### 4.3.4 Collective flow and the Eos:

After the collision and the formation of the QGP, the pressure in the plasma drives its expansion and cooling. Pressure gradients give rise to changes in the velocity distribution and the collective motion of the plasma which in turn characterize the dynamical spatial and momentum correlations of the particles in the plasma. The collective motion of the plasma driven by the internal pressure is referred to as *collective flow*. This flow provides information on the equation of state (Eos) of the plasma as is manifest in the hydrodynamic description described in section 4.1.1 above.

The collective radial expansion of the plasma is typically assessed by looking for deviations of momentum distributions from thermal although perhaps a more clear assessment is obtained by comparing spectra of particles with different masses [77].

If the transition from the QGP to the hadron gas phase is first order and occurs in LTE, then the two phases coexist at the same temperature and pressure is constant through the transition (through the Maxwell construction). However the ratio of pressure to energy density decreases and reaches a *minimum* at a particular energy density  $\varepsilon_{sp} \sim 1.4 \text{ GeV}/\text{fm}^3$  known as the *softest point of the EoS* [78]. As the energy density passes through the softest point the effective speed of sound becomes anomalously small, and the small pressure cannot accelerate effectively the matter and the flow stalls. There is a host of numerical simulations based on dynamical transport approaches that predict noticeable variations in collective flow for different equations of state (see for example [77, 78]).

The measurement of collective flow and an assessment of the EoS is an integral part of the experimental program at SPS and RHIC. There are already interesting results that prove the viability of the study of flow to understand the dynamical evolution of the hadronic component [79]. But while there is an important and exciting body of results from SPS and some recent results from STAR at RHIC [79] it is still rather difficult and perhaps premature to extract clear information on the nuclear EoS.

The main point to bear, however, is that the EoS is *experimentally accessible through measurements of flow*. Hence the experimental program in relativistic heavy ion collisions has access to the EoS which as described above is a very important aspect of the QCD phase transition.

#### 4.3.5 Other predictions...

There are a variety of other “predictions” that purport to describe potentially observable signatures of a QGP and we mention here a few that could also be of potential relevance for early Universe cosmology.

As mentioned above, there are *two* phase transitions occurring at about the same temperature, the confinement-deconfinement and the chiral symmetry breaking phase transition. Most of the observables described above refer to the confinement-deconfinement phase transition. The chiral phase transition refers to the breaking of the (approximate) symmetry corresponding to independent rotations of the right and left handed components of the u,d quarks. The three pions are the (quasi) Goldstone bosons resulting from the breakdown of chiral symmetry.

If the chiral phase transition occurs out of equilibrium, it is conceivable that strong fluctuations of the pion field could emerge. These fluctuations had been given the generic name of “disoriented chiral condensates” (or DCC’s) [80] and while there could be different manifestations of these DCC’s, all bear in common the notion of large amplitude, coherent pion “domains”. These large fluctuations would result in large regions in which isospin and probably charge are correlated. Furthermore if these domains are produced via long-wavelength (spinodal) instabilities, such as those mentioned within the context of a supercooled phase transition in section 3.1 above (see the discussion below eqn. (3.12)) there could be a host of observables associated with these domains: anomalous distribution of pions at small transverse momentum, enhanced production of direct photons with a distinct polarization asymmetry (net helicity) and strong fluctuations in the particle multiplicity on an event by event basis [81]. All of these are potentially important phenomena if they occur during or after the QCD phase transition in the early Universe. Because the pions are pseudoscalar particles, if they are produced coherently through spinodal decomposition and they eventually produce photons, this could give rise to primordial magnetic fields with *net helicity* because of the polarization asymmetry of the produced photons. This possibility, however, must be analyzed further for a reliable assessment.

There has been a substantial experimental effort by the WA98 collaboration at SPS-CERN and by the Minimax collaboration at the Tevatron (Fermilab) to detect the signatures associated with DCC’s, but so far the search has yielded negative results [82]. Furthermore, recently the NA44 collaboration at SPS-CERN has reported its experimental study of critical fluctuations on an event-by-event basis in  $Pb + Pb$  collisions. The analysis of the data does not reveal any large fluctuations that could be associated with critical phenomena.

These results disappointing as they may be should not be interpreted, yet, as the implausibility of the physical mechanism. It is conceivable that the temperature region probed by SPS is not high enough to



lead to a strongly out of equilibrium chiral transition, which would be needed for the above mechanism to be viable [81].

Thus the study of critical fluctuations and the possibility of large pion domains will be continued at RHIC.

#### 4.4 Little bang vs. Big Bang:

Having reviewed the standard Big Bang cosmology and the experimental effort to study the QCD phase transition(s) and to map the QCD phase diagram with accelerators, we now compare the settings for the QCD phase transition during the Big Bang to that prevailing in accelerator experiments, i.e, the “little bang”. The QCD phase diagram and the different regions studied with accelerator experiments as well as the region of temperatures and chemical potential prevailing during the first  $\mu\text{sec}$  after the Big Bang is depicted in figure (9) (for details on the CS (color superconducting) phase(s) see [47]). For a thorough review of the experimental aspects to study the phase diagram see [35].

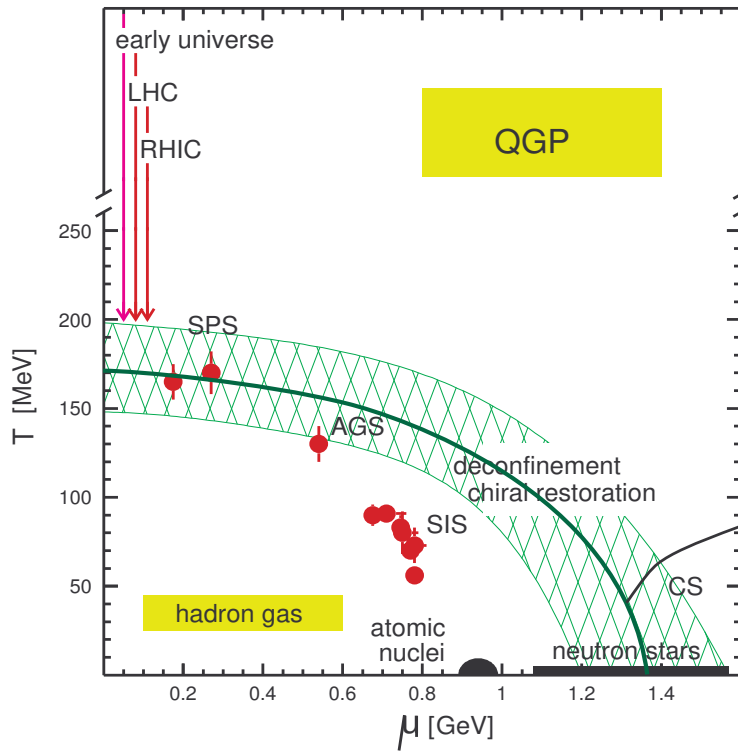


Figure 9: QGP phase diagram. Adapted from [35]

There are important similarities as well as differences between the situations in which the QCD phase transition occurs in the early Universe and in accelerators which are worth summarizing.

- **Space-time scales:** The space-time scales are very different: in the early Universe the QCD phase transition occurred at  $t \sim 1 - 10 \times 10^{-6}$  secs after the Big Bang when the size of the horizon was  $d_H \sim 10$  Km the expansion rate was  $H \sim 10^6 \text{ secs}^{-1}$ . Quark and gluon mean free paths are of order  $\sim 1$  fm, hence conditions for LTE prevailed.

In the present Universe, i.e, in heavy ion collision experiments, the lifetime of the QGP is estimated to be  $\sim 10 \text{ fm}/c$  and the typical size is  $\sim 10 \text{ fm}$ , the expansion time scale is  $\sim 1c/\text{fm}$  while the

mean free paths are still of order  $\sim 1fm$ . Therefore departures from LTE and non-equilibrium effects could play an important role in heavy ion collisions, while in the early Universe LTE is a very good approximation.

- **Baryon density:** In the early Universe, the QCD phase transition occurred in an almost baryon free environment. This is because the entropy was dominated by photons (and neutrinos) with a baryon to entropy ratio  $n_B/s \sim 10^{-9}$ . At RHIC and LHC energies it is expected that the central collision (central rapidity) region will be almost baryon free, with most of the baryons in the fragmentation regions and the entropy dominated by (almost massless) pions with a very small ratio  $n_B/n_\pi$  in the central region.
- **LSS,CMB...freeze out,HBT** There is a direct analogy between photon decoupling, the last scattering surface (LSS) in cosmology and the freeze-out of hadrons: in the case of photon decoupling, the mean free path for Thompson scattering becomes of the same order as the Hubble radius and the photons consequently free-stream. A similar situation occurs for hadrons, when their mean free path becomes larger than the typical separation of hadrons, there is no further rescattering and the hadrons free stream towards the detector. Just as in the case of the CMB where correlations in the temperature anisotropies averaged over the sky give information on the last scattering surface, there is a similar technique for hadrons, mainly pions, which makes use of the Hanbury-Brown-Twiss (HBT) interferometric effect [84, 85, 21]. Consider a source that emits *identical* particles from positions  $P_1$  and  $P_2$  and these particles are later observed at points  $P_3$  and  $P_4$  as envisaged in fig. (10). Because of the symmetrization of the pion wavefunctions, both emission points contribute to the observable at both reception points, even if the particles are non-interacting. The correlations in the momenta of the two pions are studied by defining

$$C(\vec{p}, \vec{q}) = \frac{\mathcal{P}_2(\vec{p}, \vec{q})}{\mathcal{P}_1(\vec{p})\mathcal{P}_1(\vec{q})} \quad (4.15)$$

with  $\mathcal{P}_2(\vec{p}, \vec{q})$  the joint probability of two pions with momenta  $\vec{p}$  and  $\vec{q}$  respectively and the  $\mathcal{P}_i$  are the individual probabilities, so that if  $C(\vec{p}, \vec{q}) = 1$  the events are uncorrelated.

The Fourier transform of  $\mathcal{P}_2$  gives information on the space-time structure of the source that emitted the pions [84, 85, 21]. Thus by studying pion interferometry in heavy ion collisions one learns about the space-time structure of the hadronic gas at the freeze-out surface, just as the multipole expansion of the correlation function of the temperature anisotropies gives information about the cosmological parameters at the last scattering surface [1]. In particular HBT interferometry can be used to study signals from a first order phase transition as well as coherent pion production (DCC's) [85] and is therefore an important diagnostic tool for observable consequences of the QCD phase transition(s), just as the analysis of the temperature anisotropies in the CMB.

## 4.5 QGP in the core of pulsars:

Although I have focused the discussion of observable consequences of the QCD phase transition on the experimental signatures at SPS and RHIC, corresponding to a *hot* QGP, in section 3.7 I have presented arguments suggesting that the core of neutron stars may have a deconfined phase of quarks and gluons. In neutron stars the typical temperatures are of order 1 MeV while the baryochemical potential is of order  $\sim$  GeV. Therefore a deconfined phase of quarks and gluons in this case corresponds to a cold degenerate QGP [43, 44, 48].

In a non-rotating neutron star, the boundary between the deconfined, mixed (hadron and QGP) and hadronic phases are fixed, but in a rotating neutron star (pulsar) these boundaries change as the rotational frequency of the star changes in time. In ref. [86] it was pointed out that since the compressibility of normal nuclear matter phase and the deconfined (almost free Fermi gas) of the QGP are *different* (the

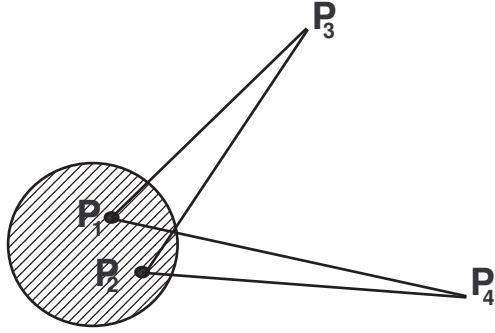


Figure 10: HBT interferometry.

incompressibility of normal nuclear matter is greater than that of an almost free Fermi gas of quarks) a structural change will occur upon a change in frequency. This has important consequences in the spin-up or spin-down stages of millisecond pulsars [86, 48]. As a millisecond pulsar spins-down, its central density may rise above the critical density for the QGP phase transition in dense nuclear matter and the central core changes to a phase with a softer equation of state. In ref. [48] the argument is reversed to contemplate the spin-up stage of a X-ray pulsar in an low-mass X ray binary (LMXB's). In this case the X-ray pulsar accretes mass from its binary companion which is typically a low mass white dwarf, and spins-up. In this case if the density at the core *falls below* the critical density the, QGP at the core turns into the hadronic phase and the existing quark matter at the core is “spun-out”. In this case, the frequency of these X-ray pulsars *increases* during accretion [48]. The authors of ref. [48] argue that for a range of frequencies the changes in the quark matter composition at the core will *inhibit* changes in the rotation frequency of the pulsar because of the increase in the moment of inertia. The net result of ref. [48] is that these accreters will spend more time near these critical frequencies resulting in an anomalous distribution of frequencies at or near this frequency. A recent analysis of the oscillations of millisecond pulsars by the Rossi X-ray Timing Explorer (RXTE) [87] clearly shows that there is a frequency,  $\sim 300$  Hz at which the pulsar distribution peaks. A detailed study of the time evolution of the moment of inertia and the rotational frequency for an LMXB was performed in ref. [48]. For the case in which the core of the pulsar has a deconfined QGP phase the authors show that the pulsar distribution has a spike at a frequency which is compatible with the RXTE data. The observed and theoretical distributions in frequency are shown in the figure (11) below.

Glendenning and Weber [48] argue that a degenerate quark matter core (cold and dense QGP) in the pulsars of some LMXB's of suitable masses can resist spin-up through the ongoing reduction of the quark matter cores in these accreting pulsars. As explained by these authors, a conversion from the *quark to hadronic* matter (the inverse situation as envisaged from a cooling QGP) manifests itself in an expansion of the star and a significant increase in the moment of inertia. The angular momentum added to the pulsar via accretion is used up by the star's expansion, inhibiting the spin-up until all the quark matter in the core has been transformed into the mixed (or hadronic) phase.

These authors conclude that while there are several possibilities to explain the spike in the frequency distribution, this mechanism can contribute to explaining the anomalous frequency distribution.

Other potential signals of a quark-hadron phase transition in neutron stars had been suggested, such as changes in the surface temperature [88] as well as rotational mode instabilities [89]. This wealth of potential observables can provide a definite *astrophysical* evidence of a deconfined phase of quarks and gluons in some of the most extreme environments in the *present* Universe.

As mentioned above, there are fascinating novel color superconducting phases that are conjectured to arise in cold and dense QCD. The observational aspects of these novel phases of QCD are still being investigated

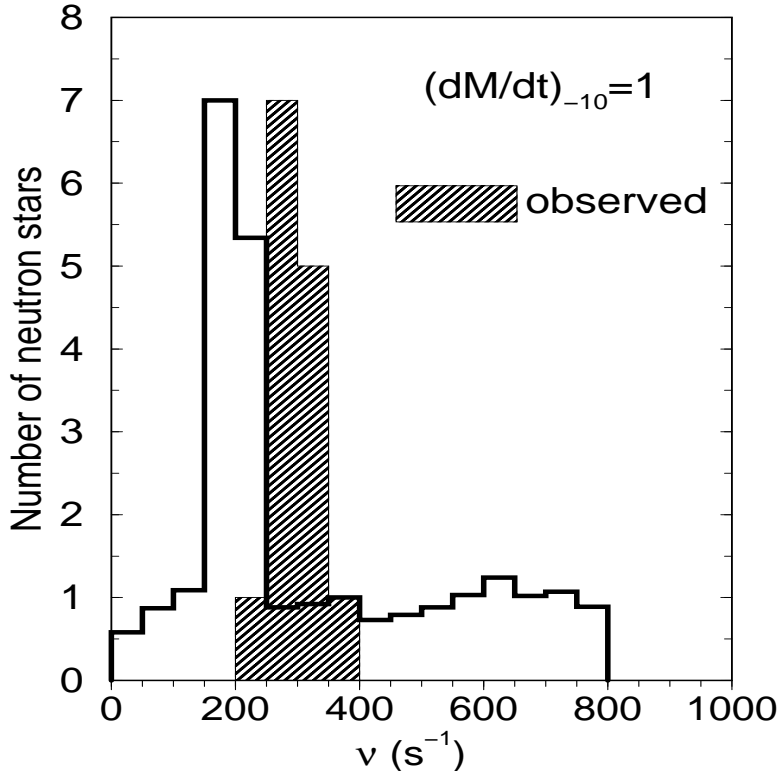


Figure 11: Frequency distribution of X-ray neutron stars. The spike in the calculated distribution is associated with the spinout of the quark matter phase and the corresponding growth of the moment of inertia. From reference [48]

and we refer the reader to the review articles in the literature ([47]) for details.

## 5 Back to the early Universe: summary

The main goal of these lectures is to assess the observational possibilities of phase transitions in early Universe cosmology. I argued that the analysis of CMB anisotropies can reveal information on phase transitions that occurred during inflation.

Phase transitions during the inflationary epoch modify the power spectrum of the primordial density fluctuations whose wavelengths cross the horizon during inflation and re-enter after recombination. Current theoretical models suggest that such phase transition occurred at a grand unified energy scale or perhaps within some supersymmetric theory but certainly beyond the current standard model and within a realm that neither theory nor experiment is on solid grounds.

I have then narrowed the discussion down to the phase transitions predicted by the standard model of particle physics because this model is on solid theoretical and experimental footing. However the observational consequences of phase transitions are argued to be rather indirect.

The standard model predicts *two* phase transitions, one at the electroweak (EW) scale and the other at the QCD scale. The latter can actually be *two* phase transitions: a confinement-deconfinement PT between an almost free gas of quarks and gluons and hadrons and the other the chiral phase transition, both at a temperature  $T \sim 150 - 200$  Mev. While originally it was conjectured that baryogenesis could be explained by a strong first order phase transition at the EW scale, current bounds from LEP for the Higgs mass seem to

rule out a strong first order phase transition. Furthermore, the magnitude of the CP violating parameters in the standard model, contained in the phase of the CKM matrix seem to be too small to lead to the observed baryon asymmetry. Thus, within the standard model the *only* phase transition that could lead to observable consequences are those of QCD. The QCD phase transition(s) occurred at a time  $t \sim 10^{-5} - 10^{-6}$  seconds after the Big Bang when the size of the horizon is  $d_H \sim 10$  Km and the mass contained within the horizon is  $\sim 1 M_\odot$ . There are several possible consequences of the QCD phase transition that have been reviewed: i) Inhomogeneous nucleosynthesis, which could lead to a possible explanation of the new constraints for  $\Omega_b h^2$  from the Boomerang/Maxima data analysis, solar mass primordial black holes, that could be part of the cold dark matter and strange quark nuggets or strangelets that can also be a component of CDM. All of these proposals are based on a first order phase transition and the details require a deep knowledge of the QCD parameters and equation of state. The lattice gauge theory program is providing reliable data on these issues but clearly there is a need for an experimental program to understand the feasibility and reliability of these observables. The experimental study of the EW phase transition itself is not feasible within our lifetime (certainly mine!) since energy densities ten orders of magnitude larger than that in nuclear matter are required. However the QCD phase transition(s) require energy densities a few times that of nuclear matter and are currently being studied by accelerators at CERN (SPS) and BNL (RHIC) with a forthcoming upgrade at CERN(LHC).

Furthermore, after an excursion into the lives and deaths of stars I presented recent results that suggest that a deconfined phase of quarks can exist at the cores of neutron stars.

I then summarized the program of relativistic heavy ion collisions that seeks to map the phase diagram of QCD and provided the recently reported analysis of “evidence” gathered at the SPS-CERN. While the interpretation of this evidence does not uniquely point to the discovery of a novel form of matter: the quark-gluon plasma (QGP), thus proving the confinement-deconfinement phase transition in QCD, taken together they represent a formidable body of “circumstantial evidence” in its favor.

From the experimental data on  $J/\Psi$  suppression as well as photons and dileptons we will learn about the physics of the deconfined hot quark gluon plasma phase as well as the hot hadron phase. From data on strangeness production we can learn about the formation of strangelets during the QCD phase transition in the early Universe. From flow we can learn the Eos of QCD and if coherent pion domains are formed and measured we can then provide a more sound assessment on the possibility of primordial magnetic fields with net helicity seeded by the decay of these coherent pion domains. Thus the experimental program will undoubtedly lead to a firmer physical picture and a more solid basis for theoretical work.

Furthermore, recent astrophysical observations of the frequency distribution of pulsars, which show an anomalous spike at  $\sim 300$  Hz *could* in fact already be a telltale signal of a novel phase of cold and dense QCD in which deconfined quarks and gluons make up the core of pulsars.

After SPS shuts down paving the way to the LHC, the torch is passed on to the Relativistic Heavy Ion Collider at BNL and the future LHC at CERN in which the ALICE program will study heavy ion reactions. Experiments at these colliders have the potential for understanding the details of the QCD phase transitions. Current and future astrophysical observations of X-ray spectra, timing and rotational properties of pulsars could confirm the possibility of deconfined quark matter at the core of these compact stars. Thus, indeed RHIC, LHC and pulsars are opening a window to the early Universe and giving a glimpse of its infancy when it was only  $10^{-6}$  seconds young.

**Acknowledgements:** The author thanks NSF for support through grants PHY-9605186, PHY-9988720 and NSF-INT-9815064.

## References

- [1] Michael S. Turner, astro-ph/9904051 (To be published in The Proceedings of Particle Physics and the Universe (Cosmo-98), edited by David O. Caldwell (AIP, Woodbury, NY); astro-ph/9901168, (To be published in the Proceedings of Wein 98 (Santa Fe, NM; June, 1998), eds. J.M. Bowles, P. Herczog and

- C. Hoffman (World Scientific, Singapore)); Michael S. Turner and J. Anthony Tyson, Rev.Mod.Phys. **71** S145 (1999); M. Kamionkowski and A. Kosowsky, Ann. Rev. Nucl. Part. Sci. **49**, 77 (1999).
- [2] G.F. Smoot et. al., Astrophys. J. **396** L1 (1992); C. L. Bennett et. al. Astrophys. J. **464** L1 (1996).
- [3] E. W. Kolb and M. S. Turner, *The Early Universe*, Addison Wesley, Redwood City, C.A. 1990.
- [4] P. Coles and F. Lucchin, *Cosmology*, J Wiley, Chichester, 1995.
- [5] A. Linde, *Particle Physics and Inflationary Cosmology*, (Harwood Academic, 1990).
- [6] A. R. Liddle and D. H. Lyth, *Cosmological Inflation and Large Scale Structure* (Cambridge University Press, 1999).
- [7] A. R. Liddle, “The Early Universe”, in “*From quantum fluctuations to cosmological structures*” eds D Valls-Gabaud, M A Hendry, P Molaro and K Chamcham, Astronomical Society of the Pacific Conference Series, Vol. **126**, 31 (1997).
- [8] D. Boyanovsky and H J de Vega, in the Proceedings of the VIIth. Erice Chalonge School on Astro-fundamental Physics, N. Sánchez ed., Kluwer, Series C, 2000, astro-ph/0006446. D. Boyanovsky, H. J. de Vega and R. Holman, Phys. Rev. **D49**, 2769 (1994). D. Boyanovsky, D. Cormier, H. J. de Vega, R. Holman, A. Singh, M. Srednicki, Phys. Rev. **D56**, 1939 (1997). D. Boyanovsky, D. Cormier, H. J. de Vega and R. Holman, Phys. Rev. **D55**, 3373 (1997).
- [9] D. Boyanovsky, D. Cormier, H. J. de Vega, R. Holman and S. P. Kumar, Phys. Rev. **D57**, 2166 (1998).
- [10] D. Boyanovsky, D.-S. Lee and A. Singh, Phys. Rev. D **48** 800 (1993).
- [11] A. Guth and S. Y. Pi, Phys. Rev. **D32**, 1899 (1985).
- [12] D. Boyanovsky, H. J. de Vega and R. Holman, “Non-equilibrium phase transitions in condensed matter and cosmology: spinodal decomposition, condensates and defects”. *Lectures delivered at the NATO Advanced Study Institute: Topological Defects and the Non-Equilibrium Dynamics of Symmetry Breaking Phase Transitions*, (Kluwer Academic, Eds. H. Godfrin and Y. Bunkov) (2000).
- [13] C.L. Bennett, A. Banday, K.M. Gorski, G. Hinshaw, P. Jackson, P. Keegstra, A. Kogut, G.F. Smoot, D.T. Wilkinson, E.L. Wright, Astrophys.J.**464**L1 (1996).
- [14] J. Barriga, E. Gaztañaga, M. G. Santos and S. Sarkar, *On the APM power spectrum and the CMB anisotropy: Evidence for a phase transition during inflation?*, astro-ph/0011398 (2001).
- [15] J. Lidsey, A. Liddle, E. Kolb, E. Copeland, T. Barreiro and M. Abney, Rev. of Mod. Phys. **69** 373, (1997).
- [16] M. Trodden, Rev. of Mod. Phys. **71**, 1463 (1999).
- [17] A. D. Sakharov, JETP lett. **5**, 24 (1967).
- [18] K. Kajantie, M. Laine, K. Rummukainen and M. Shaposhnikov, Phys. Rev. Lett. **77** 2887 (1996).
- [19] OPAL Collaboration, G. Abbiendi et al. Search for the Standard Model Higgs Boson in e+e collisions at  $\sqrt{s} = 192 - 209$  GeV, hep-ex/0101014 (to appear in Phys. Lett B); DELPHI Collaboration, P. Abreu et al. Search for the Standard Model Higgs boson at LEP in the year 2000 (to appear in Phys. Lett. B), see also: “Searches for Higgs Bosons: Preliminary combined results using LEP data collected at energies up to 202 GeV” at <http://lephiggs.web.cern.ch/LEPHIGGS/papers/CERN-EP-2000-055/index.html>.

- [20] F. Karsch, E. Laermann, A. Peikert, Ch. Schmidt, S. Stickan, *QCD Thermodynamics with 2 and 3 Quark Flavours*, hep-lat/0010027 (2000); F. Karsch, Nucl.Phys.Proc.Suppl. **83**, 14 (2000); F. Karsch, *Deconfinement and Chiral Symmetry Restoration* hep-lat/9903031 (1999).
- [21] H. Meyer-Ortmanns, Rev. of Mod. Phys. **68**, 473 (1996).
- [22] B. Kämpfer, *Cosmic Phase Transitions*, astro-ph/0004403 (2000).
- [23] J. I. Kapusta, *Quark-Gluon Plasma in the Early Universe* astro-ph/0101516 (2001).
- [24] J. H. Applegate and C. J. Hogan, Phys. Rev. **D31**, 3037 (1985); J. H. Applegate, C. J. Hogan and R. J. Scherrer, Phys. Rev. **D35**, 1151 (1987); J. Ignatius, K. Kajantie, H. Kurki-Suonio and M. Laine, Phys. Rev. **D49**, 3854 (1994); *ibid* **50** 3738 (1994); G. M. Fuller, G. J. Mathews and C. R. Alcock *ibid*, **37**, 1380 (1988); R. A. Malaney and G. J. Mathews, Phys. Rep. **229**, 145 (1993); J. Ignatius and D. J. Schwarz, hep-ph/0004259.
- [25] M. B. Christiansen and J. Madsen, Phys. Rev. **D53**, 5446, 1996.
- [26] J. Ignatius and D. J. Schwarz, *The QCD phase transition in the inhomogeneous Universe* hep-ph/0004259 (2000).
- [27] K. Jedamzik and J. B. Rehm, *Inhomogeneous Big Bang Nucleosynthesis: Upper limit on  $\Omega_b$  and the Production of Lithium, Beryllium and Boron*, astro-ph/0101292 (2001).
- [28] K. Jedamzik, Phys. Rev. **D55**, R5871 (1997).
- [29] C. Schmid, D. J. Schwarz and P. Widerin, Phys. Rev. **D59**, 043517 (1999).
- [30] J. I. Kapusta, *Primordial Black Holes and Hot Matter* astro-ph/0101515 (2001).
- [31] J. Madsen, *Physics and Astrophysics of Strange Quark Matter*, astro-ph/9809032 (1998).
- [32] E. Witten, Phys. Rev. **D 30**, 272 (1984).
- [33] C. Alcock and E. Farhi, Phys. Rev. **D 32**, 1273 (1985).
- [34] U. Heinz and M. Jacob, *Evidence for a New State of Matter: An Assessment of the Results from the CERN Lead Beam Programme*, nucl-th/0002042; U. Heinz, *Hunting Down the Quark-Gluon Plasma in Relativistic Heavy Ion Collisions*, hep-ph/9902424 (1999); R. V. Gavai, *Quark-Gluon Plasma: Status of Heavy Ion Physics*, hep-ph/0003147 (2000); D. Zschesche, et. al. *Current Status of Quark Gluon Plasma Signals* nucl-th/0101047 (2001); M. I. Gorenstein, *Quark Gluon plasma signatures in nucleus-nucleus collisions at Cern Sps* hep-ph/0011304 (2000).
- [35] J. Stachel, Nucl.Phys.A**654**, 119c (1999) and nucl-ex/9903007 To be published in the proceedings of International Nuclear Physics Conference (INPC 98), Paris, France, 24-28 Aug 1998; P. Braun-Munzinger, Nucl.Phys.A**663** 183 (2000) and Talk given at the 15th International Conference on Particle and Nuclei (PANIC 99), Uppsala, Sweden, 10-16 Jun 1999, nucl-ex/9909014; P. Braun-Munzinger and J. Stachel, Nucl.Phys.A **606** 320 (1996).
- [36] J. Bernstein, L. S. Brown and G. Feinberg, Rev. of Mod. Phys. **61**, 25 (1989); D. N. Schramm and M. S. Turner, Rev. of Mod. Phys. **70**, 303 (1998); S. Sarkar, Rept. of Prog. in Phys. **59**, 1493 (1996).
- [37] S. Burles and D. Tytler, Astrophys. J. **499**, 699 (1998); S. Burles and D. Tytler, Astrophys. J. **507**, 732 (1998); K. A. Olive, G. Steigman and T. P. Walker, Phys. Rep. **333**, 389 (2000); S. Burles, K. M. Nollett and M. S. Turner, astro-ph/0008495; J. M. O' Meara, D. Tytler, D. Kirkman, N. Suzuki, J. X. Prochaska, and A. M. Wolfe, astro-ph/0011179.

- [38] P. de Bernardis et. al. *First results from the BOOMERanG experiment* astro-ph/0011469, and *Nature* **404**, 995; (2000); A.H. Jaffe et. al. *Cosmology from Maxima-1, Boomerang and COBE/DMR CMB Observations*, astro-ph/0007333; J.R. Bond et. al. *CMB Analysis of Boomerang, Maxima, and the Cosmic Parameters  $\Omega_{tot}$ ,  $\Omega_{bh}h^2$ ,  $\Omega_{cdm}h^2$ ,  $\Omega_{\Lambda}$ ,  $n_s$* , astro-ph/0011378; S. Hanany et. al. *MAXIMA-1: A Measurement of the Cosmic Microwave Background Anisotropy on angular scales of 10 arcminutes to 5 degrees*, astro-ph/0005123; A. E. Lange et. al. *First Estimations of Cosmological Parameters From BOOMERANG*, astro-ph/0005004.
- [39] For excellent textbooks on cosmology and galaxy formation, see M. S. Longair, *Galaxy Formation*, (Springer, 1998); T. Padmanabhan, *Structure Formation in the Universe*, (Cambridge Univ. Press, 1996); P. J. E. Peebles, *The Large Scale Structure of the Universe*, (Princeton Univ. Press, 1980); P. J. E. Peebles, *Principles of Physical Cosmology* (Princeton Univ. Press, 1993).
- [40] See for example: R. Kippenhahn and A. Weigert, *Stellar Structure and Evolution* (Springer-Verlag, N.Y. 1989).
- [41] S. L. Shapiro, and S. A. Teukolsky, *Black Holes, White Dwarfs and Neutron Stars* (John Wiley, 1983); D. Arnett, *Supernovae and Nucleosynthesis* (Princeton University Press, NY)( 1996).
- [42] For a recent review see: F.-K. Thielemann, F. Brachwitz, C. Freiburghaus, E. Kolbe, G. Martinez-Pinedo, T. Rauscher, F. Rembges, W.R. Hix, M. Liebendoerfer, A. Mezzacappa, K.-L. Kratz, B. Pfeiffer, K. Langanke, K. Nomoto, S. Rosswog, H. Schatz, M. Wiescher, *Element Synthesis in Stars*, astro-ph/0101476
- [43] N. K. Glendenning, *Compact Stars, Nuclear Physics, Particle Physics and General Relativity* (Springer, NY 1996).
- [44] F. Weber, *Pulsars as Astrophysical Laboratories for Nuclear and Particle Physics* (Institute of Physics Publishing, 1999).
- [45] H. Heiselberg and V. Pandharipande, *Ann.Rev.Nucl.Part.Sci.* **50**, 481 (2000); H. Heiselberg and M. Hjorth-Jensen, *Phys.Rept.* **328**, 237 (2000).
- [46] J. M. Lattimer and M. Prakash, *Phys. Rept.* **333-334**, 121 (2000); M. Prakash, J.M. Lattimer, J.A. Pons, A.W. Steiner and S. Reddy, *Evolution of a Neutron Star From its Birth to Old Age*, astro-ph/0012136; M. Prakash, I. Bombaci, M. Prakash, P. J. Ellis, J. M. Lattimer and R. Knorren, *Phys.Rept.* **280**, 1 (1997).
- [47] K. Rajagopal and F. Wilczek *The Condensed Matter Physics of QCD*, hep-ph/0011333; M. Alford, J. A. Bowers and K. Rajagopal, *Color Superconductivity in Compact Stars*, hep-ph/0009357; K. Rajagopal, *The Phases of QCD in Heavy Ion Collisions and Compact Stars*, hep-ph/0009058; M. Alford, *Color superconducting quark matter* hep-ph/0102047 (To appear in *Annu. Rev. Nucl. Part. Sci.*)
- [48] N. K. Glendenning and F. Weber, *Possible evidence of quark matter in neutron star X-ray binaries*, astro-ph/0003426.
- [49] See for example: Saurabh Jha, the High-Z Supernova Search Team *Testing Cosmic Acceleration with Type Ia Supernovae* and references therein, astro-ph/0101521 (2001).
- [50] For a more detailed and comprehensive analysis see B. P. Schmidt's contributions to this School.
- [51] J. W. Harris and B. Muller, *Ann.Rev.Nucl.Part.Sci.***46**,71 (1996); B. Muller in *Particle Production in Highly Excited Matter*, edited by H.H. Gutbrod and J. Rafelski, NATO ASI series B, vol. 303 (1993).
- [52] J. P. Blaizot, *Nucl. Phys.* **A661**, 3c (1999).



- [53] B. Muller, *The Physics of the Quark-Gluon Plasma*, Lecture Notes in Physics, Vol. 225 (Springer-Verlag, Berlin, 1985); L.P. Csernai, *Introduction to Relativistic Heavy Ion Collisions* (John Wiley and Sons, England, 1994); C.Y. Wong, *Introduction to High-Energy Heavy Ion Collisions* (World Scientific, Singapore, 1994).
- [54] X. N. Wang, M. Gyulassy, Phys. Rev. D**44** 3501 (1991); Phys. Rev. D**45**, 844 (1992); Comp. Phys. Comm. **83**, 307 (1994); K. Geiger and B. Müller, Nucl. Phys. B**369**, 600 (1992); K. Geiger, Phys. Rep. **258**, 237 (1995); X. N. Wang in *Quark Gluon Plasma 2* (Ed. R. C. Hwa, World Scientific, 1995); K. Geiger in *Quark Gluon Plasma 2* (Ed. R. C. Hwa, World Scientific, 1995).
- [55] J. D. Bjorken, Phys. Rev. D **27**, 140 (1983).
- [56] J.-P. Blaizot and J.-Y. Ollitrault, in *Quark-Gluon Plasma 1*, edited by R.C. Hwa (World Scientific, Singapore, 1990).
- [57] see for example: S.A. Bass, A. Dumitru, Phys.Rev. C**61**, 064909 (2000).
- [58] F. Karsch, E. Laermann, and A. Peikert, Phys. Lett. B**478**, 447 (2000); for a recent review of lattice data see: S. Ejiri, *Lattice QCD at finite temperature* hep-lat/0011006 (2000).
- [59] M. Gyulassy in *Quark Gluon Plasma 1* (Ed. by R. C. Hwa, World Scientific, 1990).
- [60] M. Le Bellac, *Thermal Field Theory* (Cambridge University Press, Cambridge, England, 1996); J. I. Kapusta, *Finite Temperature Field Theory* (Cambridge Monographs on Mathematical Physics, Cambridge Univ. Press, 1989).
- [61] E. Braaten and R.D. Pisarski, Nucl. Phys. B**337**, 569 (1990); *ibid.* B**339**, 310 (1990); R.D. Pisarski, Physica A **158**, 146 (1989); Phys. Rev. Lett. **63**, 1129 (1989); Nucl. Phys. A**525**, 175 (1991).
- [62] J.-P. Blaizot and E. Iancu, Phys.Rev. D**56**, 7877 (1997); Phys.Rev. D**55**, 973 (1997); D. Boyanovsky, H.J. de Vega and S.-Y. Wang, Phys.Rev. D**61** 065006 (2000); S.-Y. Wang, D. Boyanovsky, H. J. de Vega, D.-S. Lee, Phys.Rev. D**62**, 105026 (2000); D. Boyanovsky, H. J. de Vega, Phys.Rev. D**59** 105019 (1999).
- [63] J. O. Andersen, E. Braaten and M. Strickland, Phys.Rev. D**61**, 074016(2000); Phys.Rev. D**61**, 014017 (2000); Phys.Rev.Lett. **83**, 2139 (1999); J.-P. Blaizot, E. Iancu and A. Rebhan, Phys.Rev.Lett. **83**, 2906 (1999); Phys.Lett. B**470**, 181 (1999).
- [64] S. A. Bass, M. Gyulassy, H. Stoecker, W. Greiner, J.Phys. G**25**, R1 (1999).
- [65] T. Matsui and H. Satz, Phys. Lett. B**178**, 416 (1986); D. Kharzeev and H. Satz, Phys. Lett. B **334**, 155 (1994).
- [66] NA50 Collaboration, M. Abreu et. al. Phys. Lett. B **477**, 28 (2000).
- [67] NA50 collaboration, *J/psi suppression in Pb-Pb collisions at CERN SPS* hep-ex/0101052 (2001).
- [68] See the review article by Jan-e Alam, Sourav Sarkar, Pradip Roy, T. Hatsuda, Bikash Sinha, *Thermal Photons and Lepton Pairs from Quark Gluon Plasma and Hot Hadronic Matter*, hep-ph/9909267; J.I. Kapusta, P. Lichard, and D. Seibert, Phys. Rev. D **44**, 2774 (1991); *ibid.* **47**, 4171 (1993); R. Baier, H. Nakagawa, A. Niégawa, and K. Redlich, Z. Phys. C **53**, 433 (1992); P.V. Ruuskanen, in *Particle Production in Highly Excited Matter*, NATO ASI Series, Series B: Physics Vol. 303, edited by H.H. Gutbrod and J. Rafelski (Plenum Press, New York, 1992); L.D. McLerran and T. Toimela, Phys. Rev. D **31**, 545 (1985); P. Aurenche, F. Gelis, R. Kobes, and H. Zaraket, Phys. Rev. D **58**, 085003 (1998), and references therein.
- [69] CERES (NA45) Collaboration, B. Lenkeit et. al. Nucl. Phys. A**661**, 23c (1999).

- [70] J. Wambach and R. Rapp, Nucl. Phys. A **638**,171 c (1998).
- [71] J. Alam, S. Sarkar, T. Hatsuda, T. K. Nayak, and B. Sinha, hep-ph/0008074; J. Alam, S. Sarkar, P. Roy, T. Hatsuda, and B. Sinha, hep-ph/9909267.
- [72] WA98 Collaboration, M.M. Aggarwal *et al.*, Phys. Rev. Lett. **85**, 3595 (2000); nucl-ex/0006007.
- [73] Shang-Yung Wang, Daniel Boyanovsky, Phys. Rev. D **63**, 051702(R) (2001); Shang-Yung Wang, Daniel Boyanovsky, Kin-Wang Ng *Direct photons: A nonequilibrium signal of the expanding quark-gluon plasma at RHIC energies* hep-ph/0101251 (2001).
- [74] J. Rafelski and B. Müller, Phys. Rev. Lett. **48**, 1066 (1982); P. Koch, B. Müller and J. Rafelski, Phys. Rep. **142** 167 (1986).
- [75] F. Becattini, M. Gazdzicki, J. Sollfrank, Eur. Phys. J. C **5** 143 (1998).
- [76] G. J. Odyniec, Nucl. Phys. A **638**, 144c (1998).
- [77] See for example: P. Danielewicz *Flow and equation of state in heavy ion collisions* nucl-th/0009091; D. Teaney, J. Lauret and E. V. Shuryak, *Flow at the SPS and RHIC as a Quark-Gluon Plasma signature* nucl-th/0011058 (2000), and references therein; H. Sorge, Nucl.Phys. A **661**, 577 (1999).
- [78] C.M. Hung, E. V. Shuryak, Phys. Rev. Lett. **75**, 4003 (1995); D. H. Rischke and M. Gyulassy, Nucl. Phys. A **608**, 479 (1996); J.-Y. Ollitrault, Nucl. Phys. A **638**, 195c (1998).
- [79] E895 collaboration, C. Pinkenburg *et. al.* Phys. Rev. Lett. **83**, 1295 (1999); NA49 Collaboration, H. Appelshäuser *et. al.* Phys. Rev. Lett. **80**, 4136 (1998) and Nucl. Phys. A **661**, 341c (1999); NA49 collaboration A. M. Poskanzer *et. al.* Nucl. Phys. A **661**, 341c (1999); STAR collaboration, K. H. Ackermann *et. al.* nucl-ex/0009011.
- [80] J.D. Bjorken (SLAC), K.L. Kowalski, C.C. Taylor *Observing disoriented chiral condensates*, Presented at the Workshop on Physics at Current Accelerators and Superconductors, June 2 - June 5, 1993, Argonne, IL, hep-ph/9309235; J.D. Bjorken, K.L. Kowalski, C.C. Taylor, *Baked Alaska* Presented at 7th Les Rencontres de Physique de la Vallée d'Aoste: Results and Perspectives in Particle Physics, La Thuile, Italy, 7-13 Mar 1993. Published in La Thuile Rencontres 1993:507-528 (QCD161:R342:1993); S. Gavin, A. Gocksch, R. D. Pisarski, Phys.Rev.Lett.**72**,2143 (1994); H. Minakata, B.Muller, Phys.Lett.B**377**,135 (1996); J. Randrup, Phys.Rev. C**62** 064905 (2000); K. Rajagopal, F. Wilczek, Nucl.Phys. B**404** 577 (1993), K. Rajagopal, Nucl.Phys. A**566**, 567 (1994).
- [81] M. Bleicher, J. Randrup, R. Snellings, X.-N. Wang, Phys.Rev. C**62**, 041901 (2000); D. Boyanovsky, H.J. de Vega, R. Holman, Phys.Rev.D**51** 734 (1995), F. Cooper, Y. Kluger, E. Mottola, Phys.Rev.C**54** 3298 (1996); D. Boyanovsky, H.J. de Vega, R. Holman, S. Prem Kumar, Phys.Rev.D **56**, 5233 (1997); K. Rajagopal, in Quark Gluon Plasma 2, edited by R. Hwa, (World Scientific, 1995.).
- [82] WA98 Collaboration (P. Steinberg for the collaboration), Nucl.Phys.Proc.Suppl.**71**, 335 (1999); WA98 Collaboration (M.M. Aggarwal *et al.*), Phys.Lett.B; **420**, 169 (1998); WA98 Collaboration (Tapan K. Nayak *et al.*), Nucl.Phys.A **638**, 249c (1998); MiniMax Collaboration (T.C. Brooks *et al.*) Phys.Rev.D**61**,032003 (2000); WA98 Collaboration (Tapan K. Nayak *et al.*), Nucl.Phys.A**663**: 745 (2000); Minimax collaboration T. C. Brooks *et. al.* hep-ex/9608012 (1996); M. E. Convery, *A Disoriented Chiral Condensate Search at the Fermilab Tevatron* hep-ex/9801020, (Ph.D. Thesis) (1998).
- [83] M. L. Kopytine (for the NA44 Collaboration) *Search for critical phenomena in Pb+Pb collisions*, nucl-ex/0101006 (2001).
- [84] For a recent review of HBT in heavy ion collisions see: D. A. Brown *Accessing the space-time development of heavy ion collisions with theory and experiment* (Ph.D Thesis) nucl-th/9811061; S. Pratt, Phys. Rev. Lett **53**, 1219 (1984), Phys. Rev. D **33** (1986); G. Bertsch, Nucl. Phys. A **498**, 173c (1989).

- [85] S. Pratt, in *Quark Gluon Plasma 2* (Ed. R. C. Hwa, World Scientific, 1995).
- [86] N. K. Glendenning, S. Pei and F. Weber, Phys. Rev. Lett. **79**, 1603 (1997); N. K. Glendenning, Nucl. Phys. A **638**, 239c (1998); F. Weber, J. Phys. G: Nucl. Part. Phys. **25** R195 (1999).
- [87] M. van der Klis, *Millisecond Oscillations in X-Ray Binaries*, astro-ph/0001167 (to appear in the Annual Review of Astronomy and Astrophysics).
- [88] Ch. Schaab, B. Hermann, F. Weber, M. K. Weigel, Astrophys. J. **480**, L111 (1997).
- [89] J. Madsen, Phys. Rev. Lett. **85**, 10 (2000)